Renewable and Sustainable Energy Reviews 69 (2017) 1286–1302

Contents lists available at ScienceDirect

Renewable and Sustainable Energy Reviews

journal homepage: www.elsevier.com/locate/rser

A critical review on probabilistic load flow studies in uncertainty constrained power systems with photovoltaic generation and a new approach

B Rajanarayan Prusty, Debashisha Jena*

Department of Electrical & Electronics Engineering, National Institute of Technology Karnataka, Surathkal, India

ARTICLE INFO

Keywords:
Correlation
Gaussian mixture approximation
Photovoltaic generation
Probabilistic load flow
Probability density function

ABSTRACT

A power system with large integration of renewable energy based generations is inherently associated with different types of uncertainties. In such cases, probabilistic load flow is a vital tool for delivering comprehensive information for power system planning and operation. Efforts have been made in this paper to perform a critical review on different probabilistic load flow models, uncertainty characterization and uncertainty handling methods, since from its inspection in 1974. An efficient analytical method named multivariate-Gaussian mixture approximation is proposed for precise estimation of probabilistic load flow results. The proposed method considers the uncertainties pertaining to photovoltaic generations and load demands. At the same time, it effectively incorporates multiple input correlations. In order to examine the performance of the proposed method, modified IEEE 118-bus test system is taken into consideration and results are compared with univariate-Gaussian mixture approximation, series expansion based cumulant methods and Monte Carlo simulation. Effect of various correlation cases on distribution of result variables is also studied. The effectiveness of the proposed method is justified in terms of accuracy and execution time.

1. Introduction

Load flow study is a vital decision making tool in power system planning, operation and control [1]. In deterministic load flow (DLF), system conditions are characterized by input variables with a set of deterministic values and each variation in input requires a new solution. Furthermore, for an n bus system, with k different load values and non-dispatchable renewable generation, k^n load flows are required to be simulated [2]. With such a huge number of simulations, ranges for desired outcomes are obtained; but it is certainly impossible to know the probability of occurrence of a particular case. However, with known values of probability for each case, security and reliability of the system could be assessed quantitatively [3]. The solution accuracy in DLF strictly depends on the knowledge of input data. But, input data can only be known with certain accuracy [4]. In reality uncertainties are inherently associated with input data [5]. These uncertainties basically come from forecasting or measurement errors, random fluctuations of input variables and/or component outages. Renewable energy source (RES) such as photovoltaic (PV) power generation has gained an extensive popularity because it is free, abundantly available, harvests emission free power and dispersed throughout the globe [6]. PV generation is often probabilistic, with regional, seasonal and daily variations and strongly depends on solar irradiation. Such an intermittent RES and errors in modeling introduces additional uncertainty to the system by strongly disturbing the load flow pattern [7].

The aforementioned uncertainties affect long term as well as medium term system planning and day-ahead operations [8]. Since influence of these uncertainties is overlooked in DLF, methods based on uncertainty analysis have become a promising tool [9]. Probabilistic method is one such mathematical tool which is appreciated significantly in different power system areas. Application of this method to load flow study is known as probabilistic load flow (PLF) study. Here, the knowledge of random variable (RV) is highly essential. Stochastic load flow (SLF) is an alternatively used term for PLF and is generally favorable for system operational study that deals with short-term uncertainties [4,10]. Combined probabilistic and possibilistic tools are essential when historical data for certain input RVs are insufficient to define their distributions [11]. PLF can be carried out with the help of following methods:

a) Numerical and sampling methods, such as Monte-Carlo simulation (MCS), Latin hypercube sampling, uniform design sampling etc.

* Corresponding author.
E-mail addresses: b.r.prusty@ieee.org (B.R. Prusty), bapu4002@gmail.com (D. Jena).

http://dx.doi.org/10.1016/j.rser.2016.12.044
Received 17 July 2015; Received in revised form 22 November 2016; Accepted 6 December 2016
Available online 13 December 2016
1364-0321/

Nomenclature

A	total area of the photovoltaic module
$B(a, b)$	Beta function with shape parameters a and b
$C_{X,\,\mathrm{k}}$	k^{th} order cumulant of the random variable X
G_{ip}	conductance of line $i-p$
$h_{(ip)j}$	an element of H
$h_{(ip)uv}$	an element of H'
H	power transfer distribution factor matrix
H'	line outage distribution factor matrix
H^{*}	equivalent line outage distribution factor matrix
$H_{0\mathrm{d}}$	daily extraterrestrial solar radiation
H_{td}	daily global solar radiation
$I_{0\mathrm{h}}$	hourly extraterrestrial solar irradiance
I_{dh}	diffused solar radiation
I_{th}	hourly global irradiance on a horizontal plane
J_1	State vector Jacobian matrix
J_2	P|V| bus reactive power Jacobian matrix
J_3	Branch power flow Jacobian matrix
J_4	Slack bus power Jacobian matrix
k	diffused fraction
k_t	hourly clearness index
K_t	daily clearness index
K_T	temperature coefficient of photovoltaic generation efficiency
K_1	State vector sensitivity matrix
K_2	P|V| bus reactive power sensitivity matrix
K_3	Branch power flow sensitivity matrix
K_4	Slack bus power sensitivity matrix
l	total number of lines in the system
l	total number of $P\|V\|$ buses in the system
n	total number of buses in the system
N	Number of days
nr	total number of random variables
p	probability of normal system condition
p^{uv}	outage probability of line $u-v$
P_{Di}	real power demand at i^{th} bus
P_{Gi}	real power generation at i^{th} bus
P_i	injected real power at i^{th} bus
P_{i-p}	real power flow in line $i-p$ in normal operating condition
P_{PV}	real power generation of photovoltaic system
P'_{ip}	approximated real power flow in line $i-p$ considering network topology uncertainty
$P_{(ip)uv}$	P_{i-p} due to outage of line $u-v$
Q_{Di}	reactive power demand at i^{th} bus
Q_{Gi}	reactive power generation at i^{th} bus
Q_i	injected reactive power at i^{th} bus
Q_{i-p}	reactive power flow in line $i-p$
Q_{PV}	reactive power generation of photovoltaic system
r	irradiance on an inclined surface with certain inclination angle
r_{g}	ratio of hourly average to the daily average of global irradiation
T_1,T_2	parameters linked with photovoltaic generation
T_{Amb}	ambient air temperature
T_{C}	photovoltaic cell temperature
T_{R}	relation matrix between P_{i-p} and bus voltage angle δ
T_{Ref}	reference temperature
ΔT	forecasting error of photovoltaic cell temperature
v_{W}	local wind speed
V_i	complex bus voltage at i^{th} bus
$\bar{x}$	state vector of bus voltage magnitudes and angles
x^0	expected value x
x_{ip}	reactance of branch $i-p$
X	random variable
$\bar{y}$	vector including P at all buses except slack and Q at PQ buses
$\bar{y}'$	vector including Q of the P|V| buses.
$\bar{y}''$	vector including slack bus real and reactive powers.
y^0	expected value of y
Y	bus admittance matrix
$\bar{z}$	vector including real and reactive branch power flows
z^0	expected value of z
Z	bus impedance matrix
z_{ij}	i^{th} row, j^{th} column element of Z
δ_i	bus voltage angle at i^{th} bus
δ_{ip}	difference of bus voltage angles at i^{th} bus and p^{th} bus
η_{g}	photovoltaic generation efficiency
μ_X	mean value of random variable X
ϕ	local latitude
γ	surface azimuth angle
ω	local solar time/ hour angle
$\rho_{X_1X_2}$	Pearson product moment correlation coefficient between the RVs X_1 and X_2
σ_{X}	standard deviation of the random variable X
θ_{D}	current sun declination
θ_{I}	sun's angle of incidence
θ_{T}	surface tilt angle
θ_{Z}	solar zenith angle

b) Analytical methods (AMs), such as convolution method, cumulant method (CM) etc.
c) Approximate methods (APMs), such as point estimate method (PEM), unscented transformation method (UTM) etc.

Apart from the above classification, hybrid methods combining more than one of the above methods have gained additional interest as they suppress the shortcomings of individual constituting methods. MCS is the simplest straightforward technique for assessment of PLF. In AM input and output data for PLF are considered to be RVs. AMs are computationally efficient than MCS; however, the main concern is the involvement of intricate mathematical computations. The approach of APM is similar to MCS but executes lesser number of DLF calculations. Accuracy of APMs is sensitive to system complexity.

The paper is structured as follows: A complete review on PLF is presented in Section 2. Section 3 summarizes PLF formulations. The existing probabilistic models for PV generation are deliberated in Section 4. Inclusion of input dependency in various PLF methods is explained in Section 5. In Section 6, a complete sensitivity matrix based PLF model is described, PV generation data is probabilistically modeled and multivariate-Gaussian mixture approximation is applied for correlated PLF on IEEE 118-bus test system. Finally, the concluding remarks are presented in Section 7.

2. Complete review on PLF

In the past four decades PLF is being rigorously researched by many authors. In 2008, a sincere effort was made for the review on improvements and applications of PLF [12]. Though the review was mostly appreciated by succeeding researchers in the field, a few aspects were not outlined or completely ignored. Hence, a critical review overcoming the above cited pitfalls along with review of the work made after 2008 to till date is done in this paper. This paper in detail reviews on different PLF formulations, uncertainty handling methods, efforts to improve both accuracy and computational efficiency and concerns due to uncertainties pertaining to PV generations. Research on probabilistic

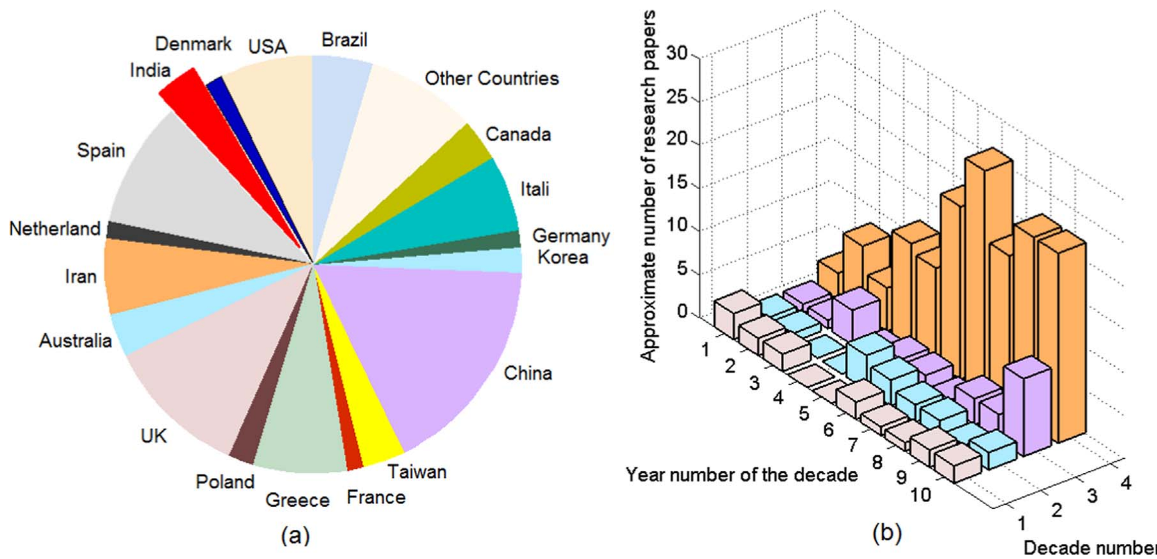

Fig. 1. Research on PLF.

optimal load flow is not taken into account in this review. Fig. 1(a) and (b) signposts country wise and decade wise (1975–2015) research contributions respectively towards PLF in the earlier four decades.

In the first decade research on PLF were mostly focused on the issues such as linearization, interdependence among nodal powers, effect of network outages etc, but the prime focus shifted to accuracy and computational efficiency in the second decade and is continued thereafter. Only a few papers with noticeable developments such as three-phase PLF in unbalanced distribution system, importance of PLF in electric traction and PLF in distribution systems with small capacity RES, were out in the third decade. Research carried out in the fourth decade mainly comprised of PLF studies to analyze impact of RES on both transmission and distribution systems, extension of existing solution methods for enhancement of accuracy and computational efficiency. A few new methods to efficiently tackle multiple objectives were also focused. The following subsections elucidate each of these issues and other related areas of PLF.

2.1. Uncertainties

The existence of uncertainty restricts the precise estimation of input variables during power system operational study and expansion planning, hence, in PLF probabilistic description of input data is required to be recognized. The sources of these uncertainties are (i) environmental and social factors and (ii) demographic and economic factors. The former is relevant to operational studies hence is called operational uncertainty whereas the latter is essential for expansion planning and hence is called planning uncertainty [13]. The basic difference between these two is the degree of information available regarding uncertainties associated with the input RVs. Uncertainties in power system can broadly be classified into input and system uncertainties.

2.1.1. Input uncertainties

Input uncertainties arise due to randomness associated with power generation and system load demand. These are discussed underneath.

a) *Generation uncertainties:* Conventional or dispatchable generator operates either in dual state or in multistate depending on the control mechanism [14]. Its randomness is often expressed in terms of forced outage rate (FOR) and follows a discrete distribution. In dual state mode, probability mass function (PMF) follows Bernoulli distribution whereas; in multistate mode it follows binomial distribution [15]. On the other hand randomness associated with non-dispatchable RESs such as PV and wind power generation is described by a continuous distribution. It mainly depends on the prime source responsible for its production such as solar irradiance and wind speed. Irradiance at a geographic location (latitude and altitude) is predictable but climatic conditions (cloud and fog); make it difficult to be precise [16]. Section 2 discusses different models available in literature for probabilistic modeling of PV generation. The probabilistic model of wind power generation is dependent on the probabilistic modeling of wind speed and wind turbine characteristics curve.
b) *Load power uncertainties:* Load is the most noticeable component in power systems. Load power is highly time dependent; comprising of both deterministic and random components. The deterministic component is repetitive and is affected by factors such as time and climatic conditions. The random component arises from forecasting and measurement errors. In the literature, two types of statistical load modeling techniques are discussed [13]. Short-term load modeling uses daily peak load power of all substations during months pertaining to peak annual load whereas; long-term load modeling uses annual peak loads at the substations for several years. Probability distribution of aggregate load power is generally ascertained from historical data. The uncertainty component arises due to environmental conditions, variations in electric appliances and customer's behavior. If the data available does not fit any functional form of distribution but is described by probability values corresponding to different range of load powers then a discrete distribution is chosen for its statistical characterization. In the absence of any historical data, Gaussian distribution is a predominant assumption. This is a reasonable representation provided the variance is not too large. The mean value of real load power is chosen as the specified deterministic value and value of standard deviation as $\pm 5\%$ to $\pm 10\%$ of the mean value. The reactive component of aggregate bus load power is modeled either in the way similar to real power modeling or is derived from the real power change assuming constant power factor [17]. When load power is forecasted precisely one-point distribution i.e. a deterministic value with probability as unity is adopted [3]. A PLF method considering non-conforming model of the system bus loads realistically models imperfect correlation [18].

2.1.2. Network uncertainties

The uncertainties associated with power system network ascend either from outage of any of its components or line parameter variations as a function of environmental factors. Each one is reviewed

Table 1
Detailed study of major contributions towards PLF.

PLF method		Ref./year	Input uncertainty: probabilistic modeling	System(s)	System model	Contributions
Numerical and sampling methods	Sampling based	[5]/1981	A: Gaussian B: Gaussian, discrete	IEEE/AEP 14-bus system	2	Inefficiency of linear model to match nonlinear model performance for higher variance of input RV is revealed.
		[43]/2009	A: Binomial B: Gaussian, discrete	IEEE 14 and 118-bus systems	3	Latin hypercube sampling into MCS provides better performance than that of simple random sampling.
		[48]/2013	B: Gaussian	IEEE 37-bus feeder	3	Higher dimensional random sample space is uniformly covered by using samples from low-discrepancy sequences.
		[47]/2014	B: Gaussian D: Weibull	IEEE 14 and 57-bus systems	3	Computational efficiency and accuracy of uniform design sampling into MCS is improved as compared to simple random sampling.
	Others	[50]/2013	A: Gaussian B: Gaussian, uniform, discrete D: Weibull E:Gaussian	New England 39-bus system	3	Linear diffusion based adaptive kernel density estimator is used for nonparametric density estimation in PLF.
		[51]/2016	A: Gaussian B: Gaussian, binomial D:Weibull F: Weibull, binomial	IEEE 14 and 118-bus systems	3	Less number of samples for desired RVs is considered and Parzen windows are applied at each point. Results are compared with various PEMs, diffusion method and MCS.
		[49]/2016	B: Gaussian D: Weibull	IEEE 30 and 118-bus systems	3	Sobol's quasi-random numbers is adopted to produce the low-discrepancy samples for MCS. Computational efficiency is improved as compared to simple random sampling and Latin hypercube sampling.
Analytical methods	Convolution based	[3]/1974	A: Binomial B: Gaussian, discrete	Typical 15 node, 26 line system	1	Information regarding line overloading probability is provided for contingency planning.
		[52]/1976	A: Binomial B: Gaussian, discrete	IEEE 14, 30, 57-bus systems	2	PDF of bus voltage magnitudes and angles, real and reactive power flows and injected reactive powers are obtained.
		[54]/1977	A: Binomial B: Gaussian, discrete	IEEE 14-bus system	2	Precise estimation of results of [52].
		[31]/1977	A: Binomial B: Gaussian, discrete	6-bus system, IEEE 14-bus system	2	Incorporates dependency between nodal power injections.
		[55]/1981	A: Gaussian B: Gaussian, discrete	IEEE 14-bus system, 32-bus system	2	Replaces convolution using LT by FFT. Results are compared with MCS.
		[36]/1984	A: Binomial B: Gaussian, discrete	New England 39-bus system	2	Linear dependency and criteria for real power balance are accounted with the help of combined COM and MCS.
		[19]/1985	A: Binomial B: Gaussian, discrete C: Discrete	IEEE 14-bus system	2	Includes network uncertainties in PLF model.
		[57]/1983	A: Binomial B: Gaussian, discrete	IEEE 14-bus system	2	Convolution based univariate-GMA is proposed to approximate multimodal desired RVs without considering input dependency.
	Cumulant based	[62]/1986	A: Binomial B: Gaussian, discrete	IEEE 14-bus system	2	Limitation of huge time consumption by LT and FFT based convolution method is overcome by proposing CM.
		[63]/2004	B: Gaussian	WSCC 179-bus test system	1	CDF of line flows are computed for reliability evaluation in expansion planning.
		[21]/2006	A: Binomial B: Gaussian, discrete C: Fictitious power injection	24-bus IEEE RTS, China 682-bus system	2	Cumulants of output RVs due to continuous and discrete input RVs are treated separately.
		[64]/2009	A: Binomial B: Gaussian D: Beta	IEEE 118-bus test system	2	The multimodal distributions of the result variables are accurately established. In order to avoid unnecessary convolutions, unimodality test is performed.
		[65]/2011	D: Weibull	IEEE 39-bus system	2	Effect of initial operating point, number of data points as well as GCM terms on PLF result is studied.
		[37]/2012	B: Modeled based on typical daily profiles D: Non-Gaussian, Gaussian	IEEE 3-bus distribution system	2	Improved voltage profile at load buses is achieved with PV generation.
		[6]/2012	B: Gaussian D: Beta	WECC 2497-bus transmission system	2	Effect of correlation and PV penetration level of both bus voltage magnitude and line real power flow is analyzed.
		[35]/2014	A: Bernoulli B: Gaussian	IEEE RTS-24, 30, 57, 79, 118-systems	1	Effect of different values of correlation among aggregate bus load demands on real line power flow is studied.
		[69]/	B: Gaussian	IEEE 118-bus system		The PLF problem is solved as a bi-level problem to

(continued on next page)

Table 1 *(continued)*

PLF method		Ref./ year	Input uncertainty: probabilistic modeling	System(s) System model	Contributions
		2016	D: Weibull	2	reduce the computational burden in case of high dimensional RVs.
Approximate methods	Point estimation based	[30]/ 2005	A: Gaussian B: Gaussian, discrete C:Uniform, binary	IEEE 6, 30, 57 and 118-bus systems 3	Consideration of system parameter uncertainty in PLF study.
		[77]/ 2007	A: Binomial B: Gaussian	IEEE 14 and 118-bus systems 3	Four point estimate schemes are tested in PLF problem. $2m + 1$ scheme provides better result for more number of inputs.
		[81]/ 2013	A: Gaussian B: Gaussian, uniform, exponential	IEEE 14-bus system 3	A new PEM is proposed which employs Rosenblatt transformation to obtain more estimating points and their corresponding weights.
		[39]/ 2014	B: Gaussian D: Weibull for wind velocity, historical hourly data for PV generation modeling	Unbalanced IEEE 123-bus distribution test system 3	$2m + 1$ scheme of PEM is employed for PLF evaluation in an unbalanced distribution system with correlated renewable generation.
		[84]/ 2013	B: Gaussian D: Discrete	NETS-NYPP system, Northeast China grid 3	Field measured wind power data is used as input RV and discrete PEM is applied for PLF considering input correlation.
	Others	[83]/ 2012	B: Gaussian D: Gaussian	Wood and Woollenberg 6-bus system, IEEE 118-bus system, 574-bus distribution system 3	UTM is claimed to be accurate and efficient as compared to existing AMs. It can easily handle correlated Gaussian and non-Gaussian input RVs.
		[86]/ 2014	B: Gaussian D: Weibull	IEEE 118-bus system 3	Compared to Hong's PEM, higher order moments are obtained with higher accuracy.
		[87]/ 2016	B: Gaussian D: Weibull	25-bus system, IEEE 118-bus system 3	Taguchi's orthogonal array based PLF is accomplished by using limited deterministic solutions.

A: Conventional generation (real power), B: Load power, C: Network, D: Renewable generation, E: Voltage magnitude of conventional generator, F: Plug-in hybrid electric vehicle.
1: DC model, 2: Linearized AC model, 3: Nonlinear model.

underneath.

a) *Topology uncertainties:* In most of the PLF formulations probability of basic network topology is assumed to be unity. Hence, it neglects probability of network element outages. However, for low level of load uncertainties, inclusion of network uncertainty into the model greatly influences the solution [19]. Network topology uncertainty is generally characterized by a discrete distribution. In its first implementation inappropriate probabilistic model was the main drawback [20]. Then, distributions of desired RVs are obtained from the weighted sum of distributions corresponding to each possible network configuration [19]. For more number of configurations, computational burden increases incredibly. Another method for dealing with random line outage considers line outage being replicated by injecting a fictional power at the buses connecting the line [21]. Von Mises step function is used to deal with the discrete part of output RVs. Distribution factor method and conditional probability method are employed to account uncertainties due to component outage [10,22]. Efforts are made to solve line outage problem by piecewise linear estimates [23]. The formulation of line and transformer outages using classical optimization method is also deliberated [24]. A few contemporary optimization techniques are applied to solve single line outage problem [25–27]. Differential evolution and particle swarm optimization algorithms for post outage voltage estimation are applied to refine work on double line outage model [28].
b) *Parameter uncertainties:* Transmission parameters estimated at a specific temperature is assumed to be constant in majority of the PLF studies. Conductor temperature is influenced by branch current, ambient temperature and other environmental factors which are probabilistic in nature. The consideration of parameter uncertainty in PLF study was first proposed in the year 1993 [29]. The series admittances of the line are assumed as discrete complex RV described by Bernoulli distribution. Probability distributions of series and shunt line parameters are assumed to follow uniform and binary distribution respectively in [30].

2.2. Effect of nodal power dependency on PLF

PLF is considered incomplete and inaccurate if dependency between nodal powers is not accounted [31]. Though consideration of node power dependency is generally ignored in long-term planning, it is considered in operational studies [32]. It is often considered to be linear owing to the difficulty in modeling an accurate dependency [31]. The word correlation refers to linear dependency. Pearson product moment correlation coefficient (PMCC) is used for the estimation of correlation. On the other hand, spearman rank order correlation coefficient and Kendall rank correlation coefficient measures monotonic relationship between inputs and are more suitable to quantify tail dependencies. In addition, both give possible ways of fitting a suitable copula function to input data. The most commonly used copula families are Archimedean family (includes Gumbel copula, Clayton copula, Frank copula etc.) and elliptical family (includes Gaussian copula, student's t-copula etc.) [33]. Selection of a suitable copula function for the available data is a challenging task. Generally maximum likelihood estimation method is employed for estimation of copula function parameters and to select the optimal copula function. Most of the regular copulas such as Frank, Clayton and Gumbel are limited to bivariate cases and their application in higher dimension case is extremely a tedious work. Among the remaining Copula functions, Gaussian copula is the most commonly used. In higher dimension applications, regular copulas are very much limited. Even though a high dimensional copula function can be built, it is difficult to write its analytical expression even for a three input case [34]. In such situations pair copula model provides flexibility to handle various dependency structures. Bivariate copula functions constituting the pair copula model may come from different families of copula. The modeling scheme of the pair copula is based on the decomposition of a multivariate copula density function into a cascade of bivariate copula functions. A pair copula with nr input RVs consists of $nr - 1$ levels.

Each level has a unique root node that connects other nodes.

Aggregated load demands at different buses are positively correlated due to social and meteorological factors [35]. PV generation at adjacent locations is strongly correlated due to common effects of solar irradiation, temperature and other environmental factors. A negative correlation between PV generation and load demand is assumed because when load demand is highest (during evening), PV generation is low and vice versa. Correlation in PLF was first considered in the year 1984 [36]. The effect of various degrees of positive correlation between PV generations [6,37] and aggregate bus load powers [35] on probability distribution of desired outcomes is analyzed. A few PLF studies consider both generation and load demand correlation [6,17,38,39]. A novel analytical PLF method is proposed to consider correlation between time varying demands and non-dispatchable renewable generations [40]. Gaussian and Clayton copula cannot capture symmetric and tail dependencies accurately whereas; Frank copula closely approximates the actual data [34]. A pair copula model is proposed to capture multiple dependencies between solar, wind and load powers [41].

2.3. PLF implementation in transmission and distribution systems

PLF implementation necessitates a system model and a suitable solution method which strictly depends on whether the system type is transmission or distribution. In this context, transmission system refers to the system wherein load connected at major substations are observed as a single unit; overlooking further distribution structure [15]. Thus the system becomes simple and assuming system balance, load flow analysis is carried out on single phase basis. On the other hand, distribution system is either radial (in rural or sub-urban areas) or meshed (in urban areas), possesses high R/X value and is often unbalanced. Hence, a method developed to solve transmission system perceives distribution system as an ill conditioned one and its implementation leads to either poorly converged result or in most cases diverges. The introduction of non dispatchable PV generations in both transmission and distribution systems further increases the load flow and its handling methods more challenging. Section 3 includes the detailed review of challenges in modeling probabilistic real power generation of PV systems and its inclusion in PLF study.

2.4. PLF evaluation methods

PLF formulation confronts various issues [2]. It is assumed that output distribution is Gaussian for Gaussian inputs [4]. The extent of deviation from Gaussian distribution mainly depends on the input data and the system model. A review on implementation of PLF methods are deliberated followed by a detailed study of major contributions in Table 1.

2.4.1. Monte-Carlo simulation

MCS is a numerical method generally used for complex, nonlinear models associated with several RVs. It relies on repetitive random sampling and statistical analysis to compute the probability distributions of the desired RVs without requiring any simplification to the original nonlinear load flow equations. MCS serves as the reference method for comparison and validation of other PLF methods because of its accuracy. The number of simulations required is independent of the system size. Stopping criteria for MCS can either be a fixed number of simulations or a particular limit for the coefficient of variation. Any random selection of sample number may either be high or insufficient for the accuracy of the obtained results. However, it is appropriate to evaluate a coefficient of uncertainty to determine the convergence of MCS. A variance coefficient (β) calculation based technique is discussed to ascertain convergence of MCS. In order to obtain the required number of samples for MCS (N_S), maximum allowable error i.e. parameter β_{max} is set as less than 1% where, β_{max} is the maximum of β obtained for all the desired RVs. This approach is described clearly underneath.

In MCS, the state of each input RV is obtained by sampling. The system state is represented as, $S = [X_1, X_2, \ldots, X_{nr}]$ where, X_i is the i^{th} input RV. For 'dnr' number of desired RVs represented by $D = [D_1, D_2, \ldots, D_{dnr}]$, the estimate of the expected value of a desired RV $D = F(S)$ for a particular system state is given as,

$$\hat{E}(F) = \frac{1}{N_S}\sum_{i=1}^{N_S} F(S_i) \tag{1}$$

where, S_i is the i^{th} sampled system state, F is the value of the desired RV for i^{th} sampled system sate.

The uncertainty of the estimate in (1) is given by its variance as given by,

$$V(\hat{E}(F)) = \frac{V(F)}{N_S} \tag{2}$$

where, $V(F)$ is the variance of F, estimated as,

$$\hat{V}(F) = \frac{1}{N_S - 1}\sum_{i=1}^{N_S} (F(S_i) - \hat{E}(F))^2 \tag{3}$$

Finally, the variance coefficient β is estimated as,

$$\beta = \frac{\sqrt{V(\hat{E}(F))}}{\hat{E}(F)} \tag{4}$$

Procedure to obtain the value of N_S:

Step-1: Set N_S =2.
Step-2: Calculate β_i for $i = 1, 2, \ldots,$ dnr using (4).
Step-3: Estimate β_{max} as maximum of values of β obtained in step-2.
Step-4: If $\beta_{max} < 1\%$, stop, else N_S=N_S+1 and go to step-2.

The application of MCS in PLF requires numerous simulations which make the method unattractive for use in practical systems [5]. However, use of sampling methods such as Latin hypercube [42,43], Latin supercube [44], importance sampling [45,46] and uniform design [47] reduces the computational burden to some extent. Quasi-MCS provide better computational speed than MCS pertaining to large variance input RVs [48]. MCS based on Johnson system and Sobol's quasi-random numbers is computationally efficient compared to Latin hypercube sampling [49]. Nonparametric density estimation based PLF studies are discussed in [50,51].

2.4.2. Analytical methods

a) *Conventional analytical methods:* Conventional analytical methods (COMs) assume simplifications such as linearization of system model, independence and Gaussian input RVs [3,52–54]. COM is first applied to linearized AC load flow model and accuracy is compared with that of DLF results [52]. COM for large systems requires numerous convolution operations. The convolution is generally accomplished using Laplace transform (LT) [53]. A new discrete frequency domain convolution by applying fast Fourier transform (FFT) is proposed and found to provide fast and precise results [55]. Though, significant improvements are achieved, calculations are still extensive [56].
b) *Gaussian mixture approximation:* Gaussian mixture approximation (GMA) technique approximates both non-Gaussian and discrete input RVs by a weighted sum of Gaussian components. A convolution based GMA considering independent input RVs is first implemented for PLF [57]. It takes huge computational time to accomplish the convolution operations. Then, Gaussian mixture component reduction technique is introduced [58]. The technique can handle multiple input correlations.
c) *Sequence operation theory:* Sequence operation theory (SOT)

based framework requires the knowledge of probability sequence. When SOT is applied to PLF, PMFs of input RVs are represented by probability sequences and arithmetic operations are accomplished with the help of three standard sequence operations such as addition type convolution (ATC), subtraction type convolution (STC) and sequence multiplication operation (SMO) [59,60]. SOT is an efficient technique to deal with discrete inputs. It cannot handle correlation between input RVs. In order to overcome the demerits of SOT, dependent discrete convolution is proposed which adopts copula function to incorporate input correlation [61]. For accuracy, it requires smaller values of discrete sequence interval which increases the computational time to accomplish the convolution operations.

d) *Cumulant method:* The distribution of linear combination of several independent RVs can be obtained with the help of CM in a single simulation and the concept is well appreciated. CM was first used in the year 1986 [62]. For large systems CM is very much acceptable since computational time significantly decreases without compromising the solution accuracy. The added advantage of having known the cumulants of the distribution is that several type of series expansion methods can be used to approximate the shape of the distribution. Three most commonly used expansion methods are Gram Charlier method (GCM), Edgeworth method (EGM) and Cornish Fisher method (CFM) [63,64]. For probabilistic assessment of system planning, combined cumulant and GCM using DC model [63] and linearized AC model [65] are applied. The consideration of first few terms of GCM gives better result while the infinite series may diverge [66]. Furthermore, GCM can only be applied to unimodal distributions [62]. A real power system comprising of both continuous and discrete input RVs the probability density functions (PDFs) of the desired RVs is obtained with multiple peaks. Under such situations, GCM leads total probability value to exceed one [8]. For uncorrelated input RVs, Von Mises method gives accurate results than GCM [21]. For non-Gaussian distributions, convergence problem with GCM is observed hence, CFM is applied to deal with non-Gaussian RVs [8]. In spite of several advantages, CM formulation becomes more involved when effect of correlation is incorporated. An enhanced CM considering correlation among RVs using Cholesky decomposition is therefore introduced [67]. Attempts are made to consider correlation among input RVs in PLF using joint cumulants [6]. EGM and CFM show untrustworthy tail behavior in some cases though are accurate in most cases. Hence, not a single expansion method is a recognized upfront approach concerning the choice of a particular expansion type and deciding number of terms to consider tail region accuracy. Authors in [40] used Pearson distribution functions to approximate distributions of power flows. Maximum entropy algorithm [68] avoids the limitations of series expansion methods by optimally fitting the distribution based on its entropy. A cumulant based multiple integral method is applied for high dimensional PLF problem with reduced computational burden [69]. First-order second-moment method (based on a first order Taylor series approximation of linearized function) obtains the first two cumulants of the desired RVs considering the first two cumulants of the input RVs [70].

2.4.3. Approximate methods

a) *Point estimate method:* PEM deals with statistics of input RVs and does not need complete knowledge about distribution. It was first proposed by Rosenblueth to deal with Gaussian input RVs [71]. Accuracy and computational efficiency using PEM improves when number of input RVs are less [72]. For a practical power system, since number of input RVs involved are more, PEM based on Rosenblueth's approach is computationally burdensome. Several other improved versions of Rosenblueth's method have come up in due course of time [73–75]. Two point estimate method (2PEM) or $2m$ scheme is the simplest PEM ever used in literature [30,76]. In this scheme, $2m$ DLFs are required to be simulated for m input RVs whereas; $2m + 1$ simulations in case of 3PEM. Comparison of various PEMs indicate that $2m + 1$ scheme gives better results for higher number of input RVs whereas; $4m + 1$, $2m$ and $3m$ are computationally inefficient, suffers from degradation of accuracy and incapable to handle non-Gaussian input RVs respectively [77]. The analysis of steady state operating condition of unbalanced three-phase system is accomplished considering correlated input RVs [78]. An unsymmetrical 2PEM is implemented and found to be more effective than symmetrical 2PEM [79]. Zhao proposed point estimation in standard Gaussian space [80]. A PEM implementation using joint distribution of input RVs is applied for PLF [81]. A combined $2m + 1$ scheme and an orthogonal transformation is implemented for assessment of PLF in an unbalanced distribution system [39]. An extended $2m + 1$ scheme deals with correlated RVs in PLF study [38,82]. For large systems computational time associated with different PEMs are directly related with the number of RVs involved [83]. Point estimation-based APMs holds low accuracy for the estimation of higher order moments. Further, they require a series expansion method to approximate the distributions

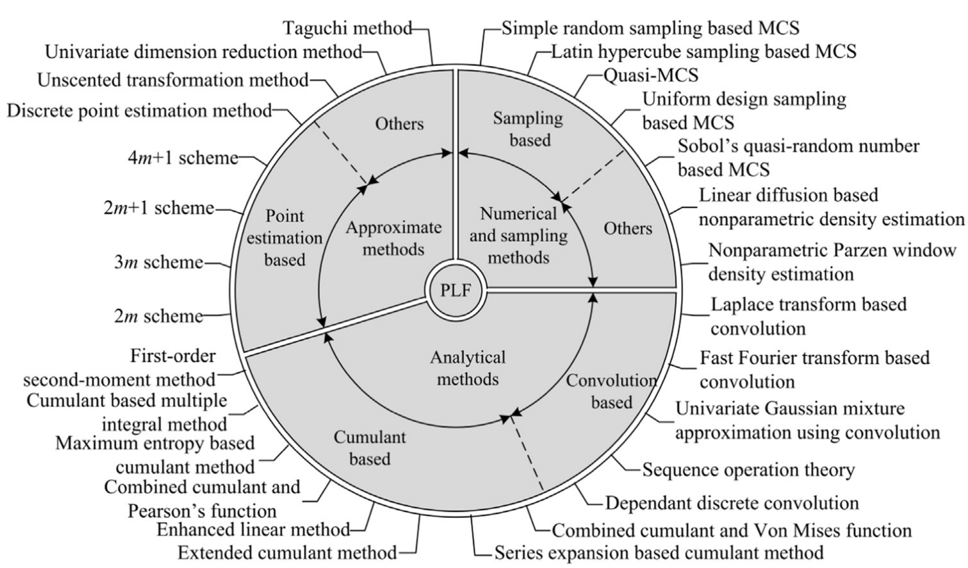

Fig. 2. Research on PLF classified by evaluation methods.

of result variables. A discrete PEM combined with GCM is applied for PLF considering field measured wind power data [84].

b) *Unscented transformation method:* The basic idea of UTM is to generate deterministically the appropriate number of samples of input RVs (referred to sigma points) by approximating their PDFs to equivalent PMFs such that both distributions have the same moments. It can easily incorporate the effect of correlation in the model accurately [83]. Conventional UTM is almost similar to that of 2PEM. Gaussian quadrature approach with conventional UTM can also be used to obtain sigma points and corresponding weights systematically [85].

c) *Other approximate methods:* Univariate dimension reduction method is employed for PLF in [86]. The first four moments are accurately estimated and distributions of the desired RVs are constructed using Johnson's system. An approximate PLF solution with a single optimal experiment is accomplished using Taguchi's orthogonal arrays [87].

2.4.4. Hybrid methods

A unified PLF for assessment of probabilistic as well as interval uncertainty (network parameters, load model coefficients) results an interval of PDFs such as lower PDF, mean PDF and upper PDF [88]. In order to account real power balance in PLF, a hybrid method combining MCS and COM is implemented [36]. The proposed hybrid method evaluates adequacy indices accurately. A hybrid method combining Markov chain Monte-Carlo and deterministic annealing expectation maximization algorithm incorporates non-Gaussian and nonlinear correlation in PLF [89]. A combined polynomial chaos expansion and nonparametric kernel density estimation obtains probability distribution of power flow responses with acceptable performance [90]. The comparison of results indicates the superiority of the method over series expansion methods. A high dimensional uncertainty problem with nonlinear dependency in PLF is solved with the combined strength of copula method and dimension-adaptive sparse grid interpolation [91]. A genetic algorithm based Latin hypercube sampling along with kernel density estimation is used to handle both positive and non-positive definite PMCC matrix in PLF [92]. Authors in [93] proposed a point estimation technique under the consideration of generator reactive power limits using spline based reconstruction method. This method accurately constructs the PDF of multimodal distributions. A combined cumulant and univariate GMA accurately approximates the multimodal distributions [94] but is computationally less efficient for increased number of discrete input RVs comprising of multiple impulses.

There are numerous methods proposed for PLF. Hence, for a quick reference research on PLF classified by evaluation methods is indicated in Fig. 2.

2.5. Three-phase PLF analysis

Unbalances in three-phase systems cannot always be negligible. The assessment of system steady state condition under uncertainty requires implementation of three-phase PLF (TPLF). TPLF was first implemented in 1997 and MCS was applied to estimate the voltage unbalance caused due to load uncertainty [95]. The interaction between unbalanced three-phase source and HVDC transmission system is studied under input uncertainty and PLF is accomplished using both MCS and linearized model [96]. TPLF in a system with unbalanced load is first discussed in the year 1999 [97]. A three dimensional joint Gaussian distribution is used for modeling of uncertainty associated with voltage unbalance [98]. The deterministic and stochastic components of three-phase real and reactive powers are modeled separately and combined MCS and network reduction theorem is used for probabilistic assessment of voltage unbalance factor [99]. The Multi-linear MCS for TPLF evaluates the PDF of phase voltage magnitudes, line flows and unbalance factors [100]. A TPLF considering correlated generation is also studied along with load uncertainty [101]. PEM is also used for TPLF studies [102,103]. Voltage regulation problem that arise due to inclusion of PV generation in distribution system is also addressed [104,105]. A TPLF is proposed to study the impact of joint correlation as well as penetration level of renewable generations on desired RVs considering asymmetrical line parameters and unbalanced load [106].

2.6. PLF in electrified railway

In electric railway systems (ERS) power consumed by a moving train (load) mainly depends on the speed and characteristics of traction equipment whereas; system configuration is ascertained from its location. The same train may also act as source during regenerative braking. Feeding systems take different form in ERS. Therefore, real and reactive power taken and supplied by the train is quite uncertain. In this type of situations PLF is a vital tool for maintenance, operation and expansion of ERS. Studies are carried out with the voltage profile of a train and feeding substation loading with the help of a simplified PLF model based on linear relationship between current in feeding as well as return conductor and train current [107]. An MCS based PLF model using train position as a RV is also addressed [108]. A similar kind of analysis was made by developing a train voltage model to express load flow equations under three different feeding systems [109].

3. Probabilistic load flow formulations

PLF study was first implemented on a DC model [2,3]. Soon after, four complex linearized formulations are deliberated [52,54]. Computation of expected values using the formulations [52] is found to be erroneous. Though the formulations [54] have precisely estimated expected values of output RVs, they are computationally burdensome. None of the formulations are able to compute distribution of real power loss. To preserve both accuracy and computational efficiency, a sensitivity coefficient based linearized formulation using Taylor's series expansion is developed [55]. A linear model accounting non-linear effects with the help of multiple linearization points is also focused [5]. Then, models incorporating the effect of correlation [31] and all possible but mutually exclusive system configurations [19] are proposed.

3.1. PLF model pertaining to numerical approach

This model is considered as an accurate model for PLF study. It is based on the concept of MCS. A detailed representation of nonlinear load flow equations is deliberated in the literature [1]. These equations are used repeatedly for different combinations of input bus powers using Newton-Raphson (NR) iterative method.

3.2. PLF models pertaining to analytical approach

3.2.1. DC model

DC load flow uses a more simplified linear form of system modeling. It is useful where fast solutions are essential, with adequate approximations. In this model, real power flow and voltage angle equations are expressed by (5) and (6) respectively.

Assumptions: $|V_i| = |V_p| = 1$ pu, $G_{ip} = 0$ and $\sin(\delta_{ip}) = \delta_{ip}$.

$$P_{i-p} = HP \tag{5}$$

$$\delta = ZP \tag{6}$$

$P_{(ip)uv}$ and P'_{ip} are given by (7) and (8) respectively.

$$P_{(ip)uv} = P_{ip} + H'P_{uv} \tag{7}$$

$$P'_{ip} = P_{ip}p + \sum P_{(ip)uv}p^{uv} \tag{8}$$

In simplest form, (8) can be expressed by (9).

$$P'_{ip} = H^{*}P \tag{9}$$

$H_{l\times n}$ and $Z_{n\times n}$ are related by the transformation given in (10).

$$H = T_R Z \tag{10}$$

An element of H and H' can be obtained using (11) and (12) respectively.

$$h_{(ip)j} = \frac{z_{ij} - z_{pj}}{x_{ip}} \tag{11}$$

$$h'_{(ip)uv} = \frac{x_{uv}(z_{iu} - z_{iv} - z_{pu} + z_{pv})}{x_{ip}\{x_{uv} - (z_{uu} + z_{vv} - 2z_{uu})\}} \tag{12}$$

This model is referred to as a large signal linear model [110].

3.2.2. Basic linearized AC model

The standard form of representation of load flow equations using non-linear functions g and h are given by (13) and (14).

$$\bar{y} = g(\bar{x}) \tag{13}$$

$$\bar{z} = h(\bar{x}) \tag{14}$$

Taylor series expansion of (13) and (14) yields (15) and (16).

$$\bar{y}_0 + \Delta\bar{y} = g(\bar{x}_0 + \Delta\bar{x}) = g(\bar{x}_0) + J_1\Delta\bar{x} \tag{15}$$

$$\bar{z}_0 + \Delta\bar{z} = h(\bar{x}_0 + \Delta\bar{x}) = h(\bar{x}_0) + J_2\Delta\bar{x} \tag{16}$$

Since $\bar{y}_0 = g(\bar{x}_0)$ and $\bar{z}_0 = h(\bar{x}_0)$, (15) and (16) can be rewritten as (17) and (18) respectively.

$$\Delta\bar{x} = J_1^{-1}\Delta\bar{y} = K_1\Delta\bar{y} \tag{17}$$

$$\Delta\bar{z} = J_3K_1\Delta\bar{y} = K_3\Delta\bar{y} \tag{18}$$

In order to preserve linearization error, J_1 is calculated once for each load flow solution [12]. This model is referred to as small signal linear model [110].

For high level of uncertainty when linearization is done at expected value of input RV, errors are reflected in the tail region of the output distribution [5]. Methods suggested to diminish this error are multi-linearized PLF (MPLF) and quadratic PLF (QPLF). In MPLF, nonlinear load flow equations are linearized around few additional points besides expected value [5]. In order to obtain the additional linearization points, a range limit is obtained using boundary load flow (BLF). A BLF algorithm based on fuzzy numbers and an optimization process was first introduced in the year 1990 [111]. Convergence problem with BLF being noticed, a new MPLF is proposed based on system real power demand [112]. On the other hand, QPLF includes a second order term of Taylor series expanded load flow equation to improve accuracy. The accuracy becomes significant when a heavily loaded system experiences large excursions [113].

4. PLF with PV generation

PLF becomes more challenging when PV generation is included in the system. Solar radiation is the prime source for PV generation and is highly uncertain. Hence, probabilistic modeling of solar radiation is necessary before ensuring PV generation modeling. PV generation in load flow study depends on the type of interconnecting bus which is modeled as PQ or $P|V|$ type. In the context of transmission systems, buses with residential roof top PV installation P_{PV} situated at vicinity to loads is generally modeled as PQ type [114]. In this case the PV generation is modeled as a negative load with fixed power levels. Reactive power capability of PV system is usually ceased due IEEE 1547 (2003) policy [115]. Since it is not a technical issue, it can be assigned either a fixed value or a value corresponding to fixed power factor [116]. On the other hand, buses connected to utility scale PV systems can be modeled as $P|V|$ type if the inverters connected to the systems have inherent reactive power capability. In this case to hold the specified voltage at the connecting bus, suitable reactive power limit is to be set. This limit corresponds to nameplate reactive limit of the inverter, which is incorporated in the load flow similar to conventional generator reactive power limit. Efforts have been made to model the real power generation of PV probabilistically. Different types of PV generation models developed in the literature are explained below.

4.1. Clearness index based modeling

The lookout of this model is to define a dimensionless expression (clearness index or atmospheric transmittance) for global solar radiation which will account for the difference between values of solar radiation measured outside the atmosphere and on the earth surface. The dimensionless expression is either K_t or k_t and is expressed by (19) or (20) respectively.

$$K_t = \frac{H_{td}}{H_{0d}} \tag{19}$$

$$k_t = \frac{I_{th}}{I_{0h}} \tag{20}$$

Clearness index cannot be predicted precisely; hence, is considered as a RV in this model. 'r'carries a non-linear relationship with k_t and the relationship is expressed as in (21).

$$r = T_1k_t + T_2k_t^2 \tag{21}$$

Expression for T_1 and T_2 are obtainable [116]. Liu and Jordan were pioneer in conducting statistical studies for k_t. They proposed Liu-Jordan rule which helps in obtaining CDF of k_t[117]. It is based on the fact that samples of solar radiation measured at different places and at different times having same μ_{k_t} will also have the same CDF for k_t. An identical model [117] is used to define PDFs of k_t[116] and P_{PV}[118]. Similar steps are followed while dealing with K_t[37]. PDFs of clearness index are unimodal [37,117] whereas; the existence of bimodal shape [119] are observed under certain situations. Accurate and complete model suitable for temperate and tropical zones is also proposed [120].

4.2. Clearness index and diffuse fraction based modeling

This model is an extension of the model discussed in Section 4.1. It incorporates randomness associated with both clearness index and diffuse fraction (describes statistical properties of diffuse irradiation). It is claimed that the above mentioned terms mainly accounts for the random effect of clouds on terrestrial irradiation [121]. 'k' is expressed as in (22).

$$k = \frac{I_{dh}}{I_{th}} \tag{22}$$

'r_g' is expressed in (23).

$$r_g = \frac{I_{th}}{H_{td}} \tag{23}$$

Using (19), (22) and (23), the RVs I_{th} and I_{dh} are given by (24) and (25) respectively.

$$I_{th} = r_gH_{0d}K_t \tag{24}$$

$$I_{dh} = r_gH_{0d}K_tk \tag{25}$$

PDF of RVs K_t[117] and k[122] are obtainable. The procedure for obtaining parameters of the PDFs is explained in the literature [37,116]. Global irradiance at an inclined surface with certain inclination angle is expressed as a linear combination of I_{th} and I_{dh} whose coefficients vary in proportion with the inclination [37]. Finally, real power generation of PV is obtained using (26).

$$P_{PV} = \eta_g rA \tag{26}$$

4.3. Global irradiance and cell temperature based modeling

This model is based on the information derived from practical data curve of PV generation [6,123]. PV generation is strongly a function of r and cell operating temperature. It is given as,

$$P_{PV} = \eta_g rA(1 - K_T \Delta T) \tag{27}$$

where, r and ΔT are RVs.

Introducing two new RVs R and T as functions of r and ΔT respectively, (27) is rewritten as,

$$P_{PV} = RT \tag{28}$$

PDF of R is modeled by beta distribution and its parameters a and b can be obtained from (29)[124,125].

$$a = \mu_R \left\{ \frac{\mu_R(1 - \mu_R)}{\sigma_R^2} - 1 \right\},\ b = (1 - \mu_R) \left\{ \frac{\mu_R(1 - \mu_R)}{\sigma_R^2} - 1 \right\} \tag{29}$$

where, σ_R is μ_R times the coefficient of variation of R.

For a solar park consisting of np number of PV units; the aggregate generation is given by (30).

$$P_{PV} = P_{PV1} + P_{PV2} + \cdots + P_{PVnp} \tag{30}$$

PDF of T is assumed to be $N\,(1\,,K_T^2 \sigma_{\Delta T}^2)$ and predictable cell operating temperature is assumed to lie within the precision limit of $\pm 5^0 C$[6].

4.4. Radiation-power curve based modeling

The basic idea of radiation-power curve based modeling is to obtain real power output of PV system with the help of its radiation-power curve [126]. Beta distribution is assumed for solar radiation. PV generation for different input solar radiation is obtained by using the characteristic equations [124].

5. Inclusion of input dependency in various PLF methods

This section discusses the process of including input dependency in various PLF methods.

5.1. Monte Carlo simulation

The basic task in MCS is to generate random samples pertaining to all the input RVs based on their probability distributions and associated dependencies. Depending on whether the associated dependencies are linear or nonlinear, the methods implemented to generate random samples are also different. In the presence of Gaussian input RVs, Cholesky decomposition based technique is employed to obtain the correlated random samples. On the other hand, for a mixture of Gaussian and non-Gaussian input RVs, two well established techniques such as Nataf transformation, polynomial normal transformation are suitable [127]. Copula function based techniques are suitable for modeling nonlinear dependency between input RVs. It separates the multivariate joint distribution into marginal distributions and the dependency structure.

5.2. Analytical methods

The primary requirement for the application of an AM for PLF is a linearized load flow model where, desired RVs are linear functions of input RVs. Dependent discrete convolution method adopts copula functions to include input dependency [61]. The input correlation can be included in CM by various formulations as described in the subsequent subsections.

5.2.1. Formulation based on joint distribution

This method necessitates the availability of JPDF or JPMF of RVs. In reality, it is a cumbersome effort to obtain joint distribution of RVs [6]. Efforts have been made to construct joint distribution of RVs from their marginal distribution using copula method [128]. However, this method is more convenient for a bivariate case and becomes more intricate in a multivariate case. Nataf model and Morgenstern model are used to construct the joint distribution [129]. Morgenstern model parameter is either constant or dependent on the shape parameters of the distribution. Nataf model provides much wider range of ρ whereas; a limit on the permitted value of ρ is the main disadvantage of Morgenstern model. For two input RVs X_1 and X_2 with sensitivity coefficients a_1 and a_2, the cumulants of (31) is calculated using (32)[8].

$$Y = a_1 X_1 + a_2 X_2 \tag{31}$$

$$C_{Y,k} = \sum_{i=0}^{k} \frac{k!}{i!(k-i)!} a_1^{k-i} a_2^i C_{(k-i),i} \tag{32}$$

For number of RVs more than two, the formulation becomes more complicated [6].

5.2.2. Formulation based on orthogonal transformation

Cholesky factorization based orthogonal transformation method accurately transforms Gaussian correlated RVs into uncorrelated sets but significant error is caused when applied to multivariate non-Gaussian cases [17]. Rotational linear orthogonal transformation technique accurately estimates the cumulants of correlated non-Gaussian RVs for orders higher than two [130].

5.2.3. Enhancements to conventional cumulant method

The enhancements over the conventional CM is in the manner, the various types of input probability distributions are dealt [131], the non-Gaussian distributions are treated [132] and the input correlation is handled [67,130]. The extended cumulant method (ECM) is an elegant method for inclusion of correlation in the cumulant formulation [130]. The detailed description of the method is discussed beneath.

ECM is an extension of the conventional CM to include input correlation in PLF. Starting with a two input case, a generalization of nr correlated inputs (both Gaussian and non-Gaussian) is explained. For two linearly correlated RVs X_1 and X_2, the cumulants of (33) are obtained using (34)–(38).

$$Y = X_1 \pm X_2 \tag{33}$$

$$C_{Y,k} = A_1(k)\, C_{X_1,k} + A_2(k)\, C_{X_2,k},\ \sigma_{X_2} \ge \sigma_{X_1} \tag{34}$$

$$C_{Y,k} = C_{X_1,k} + A_1(k) A_2(k)\, C_{X_2,k},\ \sigma_{X_1} \ge \sigma_{X_2} \tag{35}$$

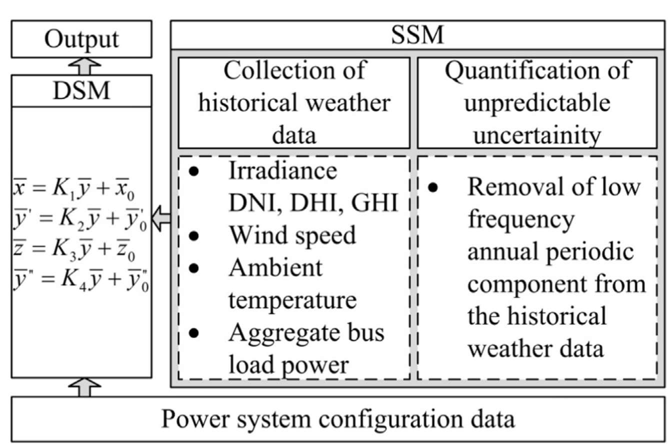

Fig. 3. Schematic approach for the assessment of PLF.

$$A_1(k) = (1+s)^k - s^k,\ A_2(k) = (\pm 1)^k \tag{36}$$

$$s = \pm \rho_{X_1X_2}\left(\frac{\sigma_{X_2}}{\sigma_{X_1}}\right),\ \sigma_{X_2} \geq \sigma_{X_1} \tag{37}$$

$$s = \pm \rho_{X_1X_2}\left(\frac{\sigma_{X_1}}{\sigma_{X_2}}\right),\ \sigma_{X_1} \geq \sigma_{X_2} \tag{38}$$

Here, s relates (36)–(38). For nonlinear dependency results obtained using this method gives an approximate value of cumulant order more than two. As a generalized case, for nr linearly correlated RVs, cumulants of (39) can be obtained using (40)–(43).

$$Y = X_1 \pm X_2 \pm X_3 \pm \cdots \pm X_{nr} \tag{39}$$

Introducing a set of RVs W_i as a sum/difference of RVs X_i and X_{i+1} (for $i = 1, 2, \ldots, nr-1$), a compact representation of (39) is given by (40).

$$Y = W_{nr-2} \pm X_{nr} \tag{40}$$

For any new RV W_i given by (41), standard deviation of W_i and PMCC between W_i and X_{i+2} are given by (42) and (43) respectively.

$$W_i = W_{i-1} \pm X_{i+1},\quad 1 \leq i \leq nr - 2 \tag{41}$$

where, $W_0 = X_1$

$$\sigma_{W_i} = \sqrt{\sigma_{X_i}^2 \pm 2\rho_{X_iX_{i+1}}\sigma_{X_i}\sigma_{X_{i+1}} + \sigma_{X_{i+1}}^2} \tag{42}$$

$$\rho_{W_iX_{i+2}} = \frac{\rho_{X_iX_{i+2}}\sigma_{X_i} \pm \rho_{X_{i+1}X_{i+2}}\sigma_{X_{i+1}}}{\sigma_{W_i}} \tag{43}$$

Finally, the distributions of desired RVs, with known values of its cumulants are approximated with the help of orthogonal function based series expansion methods.

5.3. Approximate methods

PEMs proposed by Rosenblueth, Li and Harr can easily handle correlation between input RVs whereas; Hong's PEM has a strong assumption of independent inputs [77]. This drawback is later on overwhelmed by PEM combined with Gaussian transformation technique [38]. The univariate dimension reduction method along with Johnson system precisely obtains higher order moments of desired RVs [86]. Correlation is incorporated by transforming correlated inputs into independent standard Gaussian domains.

6. PLF study using Multivariate-GMA

Apart from the detailed review of PLF since 1974 to till date, the other major contributions in this paper include:

a) A complete sensitivity matrix based PLF model is developed.
b) A probabilistic model for PV generation considering weather parameters such as, irradiance, ambient temperature and local wind speed is developed.
c) Multivariate-GMA is applied for PLF study. Optimal number of mixture components are ascertained by using cluster distortion function based approach.
d) The effectiveness of the proposed method is appraised by comparing its results with those of univariate-GMA, series expansion based cumulant methods and MCS considering accuracy and execution time as the performance criteria.

6.1. Complete sensitivity matrix based PLF formulation

Power system steady state uncertainty analysis is accomplished by a unified modeling of nodal power uncertainty in the system. The modeling steps are (i) deterministic system model (DSM) which describes the functional relationships among the input RVs and desired RVs and (ii) stochastic system model (SSM) which analyzes the impact of stochastic nodal powers on the system by quantifying their unpredictable uncertainty components. A schematic approach for the assessment of PLF is indicated in Fig. 3. The detailed modeling steps are explained broadly in the ensuing subsections.

Assumptions:

1. Second and higher order derivative terms of Taylor's series expansion are ignored during the linearization of nonlinear load flow equations.
2. Network configuration and parameters are considered constant.
3. Conventional generation dispatch is not considered.

The uncertainty component vectors of $\bar{x}$, $\bar{y}$, $\bar{z}$ and $\bar{y}''$ are given as,

$$\begin{aligned}
\Delta\bar{x} &= J_1^{-1}\Delta\bar{y} = K_1\Delta\bar{y}\\
\Delta\bar{y}' &= J_2\Delta\bar{x} = J_2K_1\Delta\bar{y} = K_2\Delta\bar{y}\\
\Delta\bar{z} &= J_3\Delta\bar{x} = J_3K_1\Delta\bar{y} = K_3\Delta\bar{y}\\
\Delta\bar{y}'' &= J_4\Delta\bar{x} = J_4K_1\Delta\bar{y} = K_4\Delta\bar{y}
\end{aligned} \tag{44}$$

Using (44) the vectors $\bar{x}$, $\bar{y}$, $\bar{z}$ and $\bar{y}''$ can be written as,

$$\begin{aligned}
\bar{x} &= K_1\bar{y} + \bar{x}_0,\ \bar{x}_0 = \bar{x}^0 - K_1\bar{y}^0\\
\bar{y}' &= K_2\bar{y} + \bar{y}'_0,\ \bar{y}'_0 = \bar{y}'^0 - K_2\bar{y}^0\\
\bar{z} &= K_3\bar{y} + \bar{z}_0,\ \bar{z}_0 = \bar{z}^0 - K_3\bar{y}^0\\
\bar{y}'' &= K_4\bar{y} + \bar{y}''_0,\ \bar{y}''_0 = \bar{y}''^0 - K_4\bar{y}^0
\end{aligned} \tag{45}$$

In (45), $\bar{x}^0$, $\bar{y}^0$, $\bar{y}'^0$, $\bar{y}''^0$, $\bar{z}^0$ are known as expected valued of $\bar{x}$, $\bar{y}$, $\bar{y}'$, $\bar{y}''$, $\bar{z}$ respectively. The values of $\bar{x}^0$, $\bar{y}^0$, $\bar{y}'^0$, $\bar{y}''^0$, $\bar{z}^0$, K_1, K_2, K_3 and K_4 are obtained from the converged DLF.

Separating discrete and continuous parts of $\bar{y}$ in (45) we get,

$$\begin{aligned}
\bar{x} &= K_1\bar{y}^{D} + K_1\bar{y}^{C} + \bar{x}_0 = \bar{x}^{D} + \bar{x}^{C} + \bar{x}_0\\
\bar{y}' &= K_2\bar{y}^{D} + K_2\bar{y}^{C} + \bar{y}'_0 = \bar{y}'^{D} + \bar{y}'^{C} + \bar{y}'_0\\
\bar{z} &= K_3\bar{y}^{D} + K_3\bar{y}^{C} + \bar{z}_0 = \bar{z}^{D} + \bar{z}^{C} + \bar{z}_0\\
\bar{y}'' &= K_4\bar{y}^{D} + K_4\bar{y}^{C} + \bar{y}''_0 = \bar{y}''^{D} + \bar{y}''^{C} + \bar{y}''_0
\end{aligned} \tag{46}$$

where, $\bar{x}^{C} = \bar{x}^{G} + \bar{x}^{NG}$, $\bar{y}'^{C} = \bar{y}'^{G} + \bar{y}'^{NG}$, $\bar{y}''^{C} = \bar{y}''^{G} + \bar{y}''^{NG}$ and $\bar{z}^{C} = \bar{z}^{G} + \bar{z}^{NG}$.

The superscripts ‘D’, ‘C’, ‘G’ and ‘NG’ stands for discrete, continuous, Gaussian and non-Gaussian components respectively. In (46), the discrete and continuous components are assumed independent. The orders of different vectors/matrices involved in (46) are indicated in Table 2.

Note: Real power injections at slack bus and P|V| buses as well as reactive power injections at P|V| buses may have uncertainty components but their effect on the solution of result variables do not have any real meaning [133].

6.2. Uncertainty modeling of PV generation

The historical data for PV generation observed at three different places of United States during the period of 2012–2013 at 12 noon is shown in Fig. 4[134]. It is observed that the production pattern is

Table 2
Orders of vectors and matrices used in (45).

Vector	Order	Vector	Order	Matrix	Order
$\bar{x}$	$k^* \times 1$	$\bar{x}_0$	$k^* \times 1$	K_1	$k^* \times k^*$
$\bar{y}$	$k^* \times 1$	$\bar{y}'_0$	$m \times 1$	K_2	$m \times k^*$
$\bar{z}$	$2l \times 1$	$\bar{z}_0$	$2l \times 1$	K_3	$2l \times k^*$
$\bar{y}'$	$m \times 1$	$\bar{y}''_0$	2×1	K_4	$2 \times k^*$
$\bar{y}''$	2×1	Let $k = 2n - m - 2$			

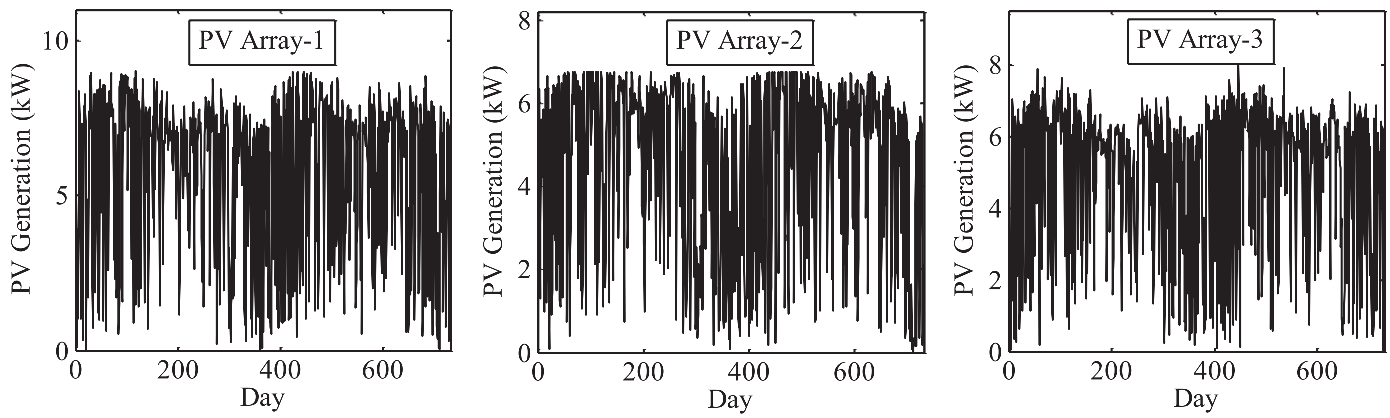

Fig. 4. Typical PV generation plots during 2012–2013.

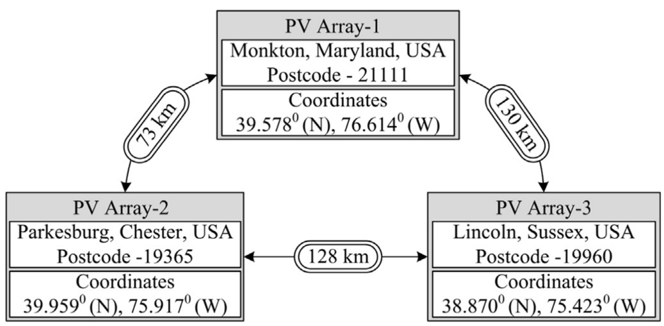

Fig. 5. Geographical details of the three cites in USA.

Table 3
Comparison of uncertainty results of PV generation.

PV Array	Mean value	Coefficient of variation	
		Observed data	After processing
1	5.7314 kW	45.43%	44.28%
2	4.5745 kW	46.09%	43.57%
3	4.8913 kW	43.26%	42.09%

periodic in nature. The unpredictable uncertainty component can be estimated by removing the deterministic periodic component (due to annual positioning of sun in the sky) [6]. The geographical details of the three places are indicated in Fig. 5. It can be observed from Table 3 that, the coefficient of variation still has higher value after processing. This indicates PV generation has high content of uncertainty.

The unpredictable uncertainty components of PV generation data can be directly used by the proposed method for PLF. In order to predict the PV generation at a future time, details regarding the parameters of the PV array, geographical location and the weather parameters such as irradiance, ambient temperature and local wind speed are required to be known.

The expression for P_{PV}[135] is given as,

$$P_{PV} = rAk_{PV}\{1 - K_T(T_C - T_{Ref})\} \tag{47}$$

where, k_{PV} is a factor which is the product of PV generation efficiency and transmittance of the PV cell's outside layer.

In (47), r is comprising of the components such as, direct tilted irradiance (DTI), reflected tilted irradiance (RTI) and diffused tilted irradiance (DITI) which are expressed as [136],

$$\begin{aligned} r &= \text{DTI} + \text{RTI} + \text{DITI} \\ \text{DTI} &= (\text{DNI})\cos\theta_I \\ \text{RTI} &= (\text{GHI})\,(\text{AP})\left(\frac{1-\cos\theta_T}{2}\right) \\ \text{DITI} &= (\text{DHI})\left(\frac{1+\cos\theta_T}{2}\right) + (\text{GHI})\left\{\frac{(0.012\theta_Z - 0.04)\,(1-\cos\theta_T)}{2}\right\} \end{aligned} \tag{48}$$

where, DNI, GHI and DHI stands for direct normal irradiance, global horizontal irradiance and diffuse horizontal irradiance respectively; Albedo parameter AP is taken as 0.2.

The expression for $\cos\theta_I$ is given as,

$$\begin{aligned} \cos\theta_I = {} & \sin\phi\,(\sin\theta_D\cos\theta_T + \cos\theta_D\cos\gamma\cos\omega\sin\theta_T) \\ & + \cos\phi\,(\cos\theta_D\cos\omega\cos\theta_T - \sin\theta_D\cos\gamma\sin\theta_T) \\ & + \cos\theta_D\sin\gamma\sin\omega\sin\theta_T \end{aligned} \tag{49}$$

In (49), θ_D is expressed as,

$$\theta_D = -\sin^{-1}[0.39779\cos\{0.98565^0(N + 10) + 1.914^0\sin(0.98565^0(N - 2))\}] \tag{50}$$

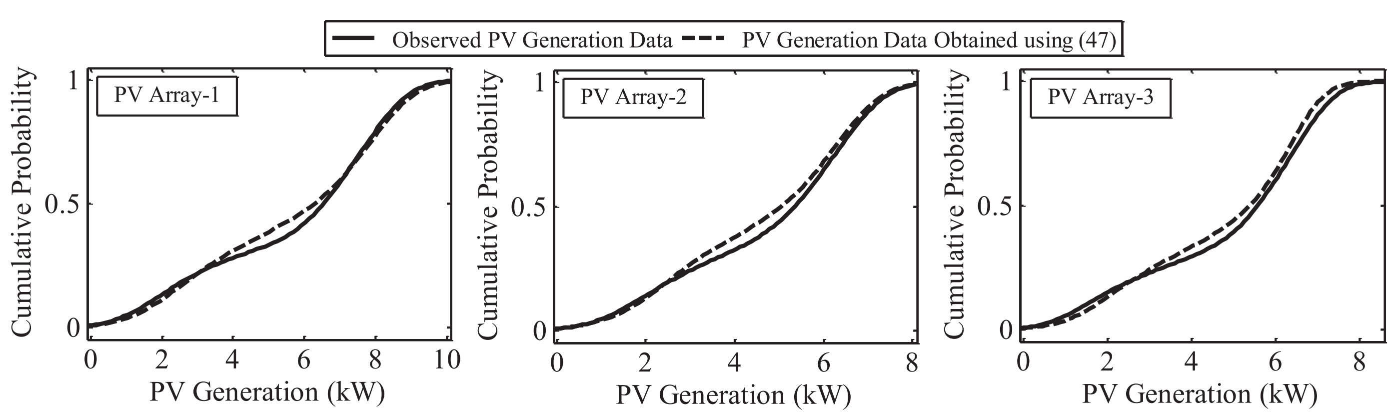

Fig. 6. Comparison of cumulative probability plots of actual PV generation data and that using (47).

Table 4
Comparison of PMCCs before and after removal of the periodic componenets.

Observed PV generation data								PV generation data using (47)			
Without processing				After processing							
	A-1	A-2	A-3		A-1	A-2	A-3		A-1	A-2	A-3
A-1	1	0.7398	0.6644	A-1	1	0.7245	0.6463	A-1	1	0.8252	0.7131
A-2	0.7398	1	0.6420	A-2	0.7245	1	0.6173	A-2	0.8252	1	0.7056
A-3	0.6644	0.6420	1	A-3	0.6463	0.6173	1	A-3	0.7131	0.7056	1

Table 5
Probabilistic description of discrete load power at bus-47.

Load power Capacity (p.u.)	Real 0.34	Probability value
Discrete values (p.u.)	0.23	0.10
	0.24	0.15
	0.36	0.30
	0.38	0.25
	0.39	0.20

The value of γ is 0^0, 45° and 90° respectively for south facing, south-west facing and west facing PV modules.

As per the empirical thermal model [123], T_C is expressed as,

$$T_C = r\, e^{k_1 + k_2 v_W} + T_{Amb} \tag{51}$$

where, $k_1 = -2.98$ and $k_2 = -0.0471$ for close roof mounted glass/cell/glass type modules.

In order to validate the PV generation obtained using the above formulation with that of the observed one, samples of weather data such as, DNI, GHI, DHI, T_{Amb} and v_W are collected from the same three locations at 12 noon [137,138]. Obtain r using (48) and T_C using (51). The annual low frequency components of r and T_C are removed from the data. The unpredictable uncertainty component of r and T_C are directly used in (47) to obtain PV generation at a future time. In (47), k_{PV} is either provided by the PV module manufacturers or its value can be obtained as,

$$k_{PV} = \frac{\mu_{P_{PV}}}{\mu_r A\left\{1 - \beta_{Ref}\left(\mu_{T_C} - T_{Ref}\right)\right\}} \tag{52}$$

The cumulative probability plots of PV generation data as obtained using (47) closely matches with that of the observed data (see Fig. 6). Average root mean square errors (ARMSEs) are estimated as 0.2694%, 0.3073% and 0.3035% respectively considering observed data as the reference.

The ARMSE is calculated as,

$$\mathrm{ARMSE} = \frac{\sqrt{\sum_{i=1}^{N_p}\left(F_{Ref\,i} - F_{Com\,i}\right)^2}}{N_p} \times 100 \tag{53}$$

where, $F_{Ref\,i}$ and $F_{Com\,i}$ respectively are the i^{th} value of cumulative probability using reference and comparing plots, N_p is the selected number of points chosen from the range of cumulative probability plot.

The PMCC between the actual PV generations and that between their unpredictable uncertainties is provided in Table 4. There is a high value of PMCC between Array-1 and 2 owing to their geographical closeness. The PMCC between Array-1 and 3 as well as between Array-2 and 3 are comparatively less and are nearly equal. It is observed that there is no significant variation in PMCC value after the removal of low frequency component (see Table 4). PV generation data obtained using (47) also has nearly the same values of PMCC.

6.3. Multivariate-GMA

GMA approximates both non-Gaussian and discrete input RVs by a weighted sum of Gaussian components. When GMA is applied to individual non-Gaussian one-dimensional RVs, it is referred to as univariate-GMA [57,94]. In multivariate-GMA, the correlated non-Gaussian input RVs at various buses are augmented together to form a multivariate structure. Multivariate-GMA includes the correlation information between the mixture components of the multivariate structure. In case of multivariate-GMA, the distribution of an nr-dimensional augmented structure y_a is given as,

$$f(y_a) = \sum_{k=1}^{g} w_k f_k(y_a, \Sigma_k) \tag{54}$$

The distribution of nr-dimensional k^{th} Gaussian function is expressed as,

Table 6
The base case PMCC matrix.

RVs	PV_1	PV_2	PV_3	P_{D101}	P_{D102}	P_{D106}	P_{D108}	P_{D109}	Q_{D101}	Q_{D102}	Q_{D106}	Q_{D108}	Q_{D109}
PV_1	1	0.825	0.713	0.3	0.3	0.3	0.3	0.3	0.3	0.3	0.3	0.3	0.3
PV_2	0.825	1	0.706	0.3	0.3	0.3	0.3	0.3	0.3	0.3	0.3	0.3	0.3
PV_3	0.713	0.706	1	0.3	0.3	0.3	0.3	0.3	0.3	0.3	0.3	0.3	0.3
P_{D101}	0.3	0.3	0.3	1	0.5	0.5	0.5	0.5	1	0.5	0.5	0.5	0.5
P_{D102}	0.3	0.3	0.3	0.5	1	0.5	0.5	0.5	0.5	1	0.5	0.5	0.5
P_{D106}	0.3	0.3	0.3	0.5	0.5	1	0.5	0.5	0.5	0.5	1	0.5	0.5
P_{D108}	0.3	0.3	0.3	0.5	0.5	0.5	1	0.5	0.5	0.5	0.5	1	0.5
P_{D109}	0.3	0.3	0.3	0.5	0.5	0.5	0.5	1	0.5	0.5	0.5	0.5	1
Q_{D101}	0.3	0.3	0.3	1	0.5	0.5	0.5	0.5	1	0.5	0.5	0.5	0.5
Q_{D102}	0.3	0.3	0.3	0.5	1	0.5	0.5	0.5	0.5	1	0.5	0.5	0.5
Q_{D106}	0.3	0.3	0.3	0.5	0.5	1	0.5	0.5	0.5	0.5	1	0.5	0.5
Q_{D108}	0.3	0.3	0.3	0.5	0.5	0.5	1	0.5	0.5	0.5	0.5	1	0.5
Q_{D109}	0.3	0.3	0.3	0.5	0.5	0.5	0.5	1	0.5	0.5	0.5	0.5	1

$$f_k(y_a, \Sigma_k) = \frac{1}{(2\pi)^{\frac{nr}{2}} |\Sigma_k|^{\frac{1}{2}}} e^{-\frac{1}{2}(y_a-\mu_k)^{\mathrm{T}}(\Sigma_k)^{-1}(y_a-\mu_k)} \tag{55}$$

where, w_k, μ_k and Σ_k are the weight factor, mean vector and covariance matrix of the nr-dimensional k^{th} Gaussian function respectively; $|\Sigma_k|$ and $(\Sigma_k)^{-1}$ are the determinant and inverse of Σ_k respectively; w_k must satisfy $0 < w_k \le 1$ and $\sum_{k=1}^{g} w_k = 1$; 'g' is the order of Gaussian sum.

The optimal value of 'g' is obtained using cluster distortion function based approach. The mixture parameters pertaining to each Gaussian component are obtained using expectation maximization (EM) algorithm.

The probability distribution of y^{D} at j^{th} bus using GMA can be approximated as,

$$f\left(y_j^{\mathrm{d}}\right) = \sum_{k=1}^{g_j'} w_{jk} f_{N_k(d_{jk},0)}\left(y_j^{\mathrm{d}}\right) \tag{56}$$

and must satisfy

$$\sum_{k=1}^{g_j'} w_{jk} = 1 \tag{57}$$

where, d_{jk} and w_{jk} are referred to as the k^{th} discrete value and its corresponding probability respectively, 'g_j''' is the discrete impulse number of y_j^{D}, $f_{N_k(d_{jk},0)}$ is the one-dimensional Gaussian distribution with mean value of d_{jk} and variance set to zero.

The total number of Gaussian components (N_{r}) essential to obtain the distribution of a desired RV using multivariate-GMA is estimated as the product of the total Gaussian component numbers pertaining to the augmented correlated non-Gaussian multivariate structures as well as discrete input RVs. PLF using multivariate-GMA follows similar steps as in univariate-GMA [94] except for the multivariate augmentation of correlated non-Gaussian RVs.

6.3.1. Cluster number selection approach

Clustering approach such as k-means requires the value of cluster number to be known a priori. A cluster distortion function-based approach is explained for the estimation of optimal number of data clusters for a given multivariate data. Here, the idea is to identify the concentrated regions of objects in the given data i.e. the data distortion. The sum of cluster distortion for a given value of 'g' is given as [139],

$$S_{\mathrm{g}} = \sum_{j=1}^{\mathrm{g}} I_j \tag{58}$$

and the function $f(\mathrm{g})$ for cluster number selection is given as,

$$f(\mathrm{g}) = \begin{cases} 1 & , \mathrm{g} = 1 \\ \frac{S_{\mathrm{g}}}{\alpha_{\mathrm{g}} S_{\mathrm{g}-1}}, & S_{\mathrm{g}-1} \neq 0 \,\&\, \mathrm{g} > 1 \end{cases} \tag{59}$$

where, I_j and S_{g} are distortion of j^{th} cluster and sum of cluster distortions for 'g' number of clusters respectively.

If data dimension $N_{\mathrm{d}} > 1$, then α_{g} in (60) is expressed as,

$$\alpha_{\mathrm{g}} = \begin{cases} 1 - \frac{3}{4N_{\mathrm{d}}} & , \mathrm{g} = 2 \\ \alpha_{\mathrm{g}-1} + \frac{1-\alpha_{\mathrm{g}-1}}{6} & , \mathrm{g} > 2 \end{cases} \tag{60}$$

and must satisfy the condition $0 < \alpha_{\mathrm{g}} \le 1$.

For smaller value of $f(\mathrm{g})$, the data is more concentrated. Hence, the value of 'g' that yields smaller value of $f(\mathrm{g})$ is regarded as optimal.

6.4. Computational procedure for multivariate-GMA

The procedures for PLF evaluation based on multivariate-GMA considering correlation among input RVs comprises of following steps:

Step-1: Estimate the optimum value of 'g' using cluster number selection approach.
Step-2: Evaluate N_{r}.
Step-3: Obtain the cluster centers using k-means algorithm.
Step-4: Execute the following for each desired RV.

(i) Obtain the mixture components of the augmented non-Gaussian structure using EM algorithm (use step-3 data for EM initialization).
(ii) Find weight vector w of N_{r} components.
(iii) Estimate equivalent mean and variance vectors M and V of N_{r} components using (46).
(iv) Approximate the probability distributions of desired RVs as the weighted sum of distributions of N_{r} Gaussian components.

6.5. Case studies and comparison of results

The cluster distortion function based multivariate-GMA is applied for PLF on modified IEEE 118-bus test system [140]. The system is consisting of 53 conventional generating units and 186 transmission branches. The system base MVA is 100 MVA. The modifications in the system are done by installing three solar parks of capacities 0.0283 p.u., 0.0222 p.u. and 0.0238 p.u. respectively at bus numbers 106, 108 and 109. The solar parks are created by combining 500 of PV arrays (see Fig. 5) in each of the respective places. It is assumed that the real and reactive power demands at buses 101, 102, 106, 108 and 109 follow Gaussian distribution. Due to constant load power factor assumptions real and reactive load powers are completely correlated. The mean values are taken as specified deterministic data and standard deviations as 10% of the mean values. The detail of discrete load power is specified in Table 5. The expected value of the discrete load power is same as that of the specified deterministic data. The PMCC matrix is decided as per Table 6 and is considered as the base case PMCC matric. The probability distribution of PV generation is multi-modal. The correlated PV generations of the solar parks are augmented to form a multivariate structure (three-dimensional). Cluster distortion function based approach is applied and the value of 'g' is obtained as 2. MCS with 30,000 samples is chosen as a comparative reference. This value is obtained by setting variance coefficient $\beta_{\max}$ less than 1% for all the desired RVs. The MATLAB programming codes are simulated on a computer with 3.4 GHz, i7 processor and RAM size of 8 GB.

The cumulative probability plots of branch power flow in the branch connecting bus numbers 37 and 40 is compared in Fig. 7. The plots are obtained considering base case PMCC matrix. Both the GMA based methods approximate the distribution curve close to MCS plot. Series expansion based cumulant methods are incapable of approximating the multimodal distributions accurately. The performance of multivariate-GMA with respect to other methods is compared in Table 7.

It is observed that multivariate-GMA takes less time to approximate multimodal distributions accurately compared to other methods including MCS. In order to perceive the effect of various correlation cases on distributions of desired RVs, three correlation conditions are decided in Table 8. Multivariate-GMA is used to obtain the distribu-

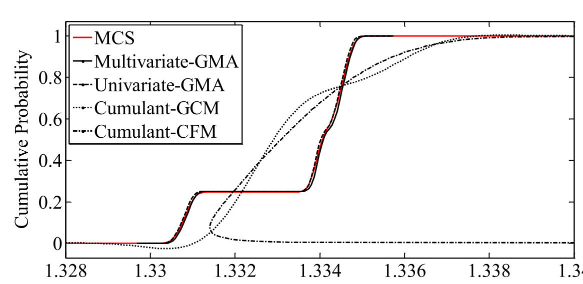

Fig. 7. Comparison of cumulative probability plots of branch power flow using various methods.

Table 7
Simulation time and accuracy comparison.

PLF method	Simulation time (sec)	Average of ARMSEs
MCS	1842.15	–
Multivariate-GMA	41.71	0.1361
Univariate-GMA	71.96	0.1403
Cumulant-GCM	60.75	0.2654
Cumulant-CFM	44.38	0.2234

Table 8
Different correlation conditions.

Correlation type	Case-1	Case-2	Case-3
PV-PV	0, 0.5, 1	Base case	Base case
PV-Load	Base case	0, 0.5, 1	Base case
Load-Load	Base case	Base case	0, 0.5, 1

Table 9
Effect of various correlation cases on $P_{L108-109}$.

Desired RV	Correlation case	PMCC	μ (p.u.)	σ (p.u.)
$P_{L108-109}$	Case–1	0	0.4644	0.0082
		0.5	0.4644	0.0079
		1	0.4644	0.0076
	Case–2	0	0.4644	0.0078
		0.5	0.4644	0.0077
		1	0.4644	0.0076
	Case–3	0	0.4644	0.0065
		0.5	0.4644	0.0066
		1	0.4644	0.0067

tions.

The effect of various values of PMCC on mean values and standard deviations of $P_{L108-109}$ pertaining to each correlation type is compared in Table 9. The impact of input correlation has noticeable effect on standard deviation and other higher order statistical moments. The effect is more prominent in the tail region of the distributions. Depending on the sign of sensitivity coefficients, the effect of input correlation either elongates or shortens the tail region of the distributions of desired RVs. The increase in PMCC value decreases the standard deviation of $P_{L108-109}$ for case-1 and case-2 correlation cases whereas, increases the standard deviation for case-3 correlation.

Further, a fixed change in PMCC value results in fixed change in standard deviation values. This is because of the linear relationship between input and desired RVs. The PMCC between the input RVs do not affect the expected values of desired RVs whereas, the standard deviation is linear function of PMCC. However, in case of nonlinear relationships, input correlation also has an effect on expected values of desired RVs.

7. Conclusions

A critical review on PLF for the last four decades is carried out. Sincere efforts are made in the review to deal with different types of uncertainties, effect of correlation, PLF evaluation methods and application of PLF to various power system areas. In order to approximate multimodal probability distributions, an efficient AM named multivariate-GMA is applied for PLF on modified IEEE 118-bus system. Correlated non-Gaussian bus powers at various buses are augmented together to form a multivariate structure. The optimal number of clusters pertaining to the multivariate data is estimated with the help of cluster distortion function based approach. The results of the k-means clustering algorithm pertaining to the optimal cluster number is used for the initialization of EM algorithm to obtain GMA parameters. The results of the proposed method are compared with that of four AMs and MCS. The proposed method accurately obtains the distributions of multimodal desired RVs in less time compared to other methods.

References

[1] Wang XF, Song Y, Irving M. Modern power system analysis. Springer; 2008.
[2] Borkowska B. Probabilistic load flow. IEEE Trans Power Appar Syst 1974;93(3):752–9.
[3] Allan RN, Borkowska B, Grigg CH. Probabilistic analysis of power flows. Proc Inst Electr Eng 1974;121(12):1551–6.
[4] Dopazo JF, Klitin OA, Sasson AM. Stochastic load flows. IEEE Trans Power Appar Syst 1975;94(2):299–309.
[5] Allan RN, Leite da Silva AM. Probabilistic load flow using multilinearisations. Proc Inst Electr Eng 1981;128(5):280–7.
[6] Fan M, Vittal V, Heydt GT, Ayyanar R. Probabilistic power flow studies for transmission systems with photovoltaic generation using cumulants. IEEE Trans Power Syst 2012;27(4):2251–61.
[7] Bloom JA. Probabilistic production costing with dependent generating sources. IEEE Trans Power Appar Syst 1985:2064–71.
[8] Usaola J. Probabilistic load flow with wind production uncertainty using cumulants and Cornish-Fisher expansion. Int J Electr Power Energy Syst 2009;31(9):474–81.
[9] Alvarado F, Hu Y, Adapa R. Uncertainty in power system modeling and computation. IEEE Int Conf Syst, Man Cybern 1992:754–60.
[10] Min L, Zhang P. A probabilistic load flow with consideration of network topology uncertainties. Int Conf Intell Syst Appl Power Syst 2007:5–8.
[11] Aien M, Rashidinejad M, Fotuhi-Firuzabad M. On possibilistic and probabilistic uncertainty assessment of power flow problem: a review and a new approach. Renew Sustain Energy Rev 2014;37:883–95.
[12] Chen P, Chen Z, Bak-Jensen B. Probabilistic load flow: a review. 3rd Int Conf Electr Util Deregul Restruct Power Technol 2008:1586–91.
[13] Leite da Silva AM, Lima JM, Ribeiro SM, Arienti VL, Schilling MT, Vieira Filho X, Soares SM. Operational and expansion planning of Brazilian systems based on probabilistic load flow. 3rd Int Conf Probabilistic Methods Appl Electr Power Syst 1991:197–202.
[14] Wang X, McDonald JR. Modern power systems planning. McGraw-Hill; 1994.
[15] Oluwabukola A. OKE, Enhanced unscented transform method for probabilistic load flow studies. [Ph.D. thesis] Submitted to University of Nottingham; 2013.
[16] Conti S, Raiti S. Probabilistic load flow using Monte Carlo techniques for distribution networks with photovoltaic generators. Sol Energy 2007;81(12):1473–81.
[17] Chen C, Wu W, Zhang B, Sun H. Correlated probabilistic load flow using a point estimate method with Nataf transformation. Int J Electr Power Energy Syst 2015;65:325–33.
[18] Stefopoulos GK, Meliopoulos AP, Cokkinides GJ. Probabilistic power flow with non-conforming electric loads. Int J Electr Power Energy Syst 2005;27:627–34.
[19] Leite da Silva AM, Allan RN, Soares SM, Arienti VL. Probabilistic load flow considering network outages. Proc Inst Electr Eng 1985;132(3):139–45.
[20] R.N. Allan, C.H. Grigg,J.A. Prato-Garcia, Effect of network outages in probabilistic load flow analysis. IEEE PES winter meeting 1979; Paper A79032-4
[21] Hu Z, Wang X. A probabilistic load flow method considering branch outages. IEEE Trans Power Syst 2006;21(2):507–14.
[22] Lu M, Dong ZY, Saha TK. A probabilistic load flow method considering transmission network contingency. Power Eng Soc Gen Meet 2007:24–8.
[23] Ruiz PA, Sauer PW. Voltage and reactive power estimation for contingency analysis using sensitivities. IEEE Trans Power Syst 2007;22(2):639–47.
[24] Ozdemir A, Lim JY, Singh C. Branch outage simulation for MVAr flows: bounded network solution. IEEE Tran Power Syst 2003;18(4):1523–8.
[25] Ozdemir A, Lim JY, Singh C. Post-Outage reactive power flow calculations by genetic algorithms: constrained optimization approach. IEEE Trans Power Syst 2005;20(3):1266–72.
[26] Ceylan O, Ozdemir A, Dag H. Branch outage solution using particle swarm optimization. Power Eng Conf 2008:1–5.
[27] Ceylan O, Ozdemir A, Dag H. Comparison of post outage bus voltage magnitudes estimated by harmony search and differential evolution methods. 15th Int Conf Intell Syst Appl Power Syst (ISAP) 2009:8–12.
[28] Ceylan O, Ozdemir A, Dag H. Double branch outage modeling and simulation: bounded network approach. Int J Electr Power Energy Syst 2015;73:369–76.
[29] Patra S, Misra RB. Probabilistic load flow solution using method of moments. 2nd Int Conf Adv Power Syst Control, Oper Manag 1993:922–34.
[30] Su C-L. Probabilistic load-flow computation using point estimate method. IEEE Trans Power Syst 2005;20(4):1843–51.
[31] Allan RN, Al-Shakarchi MRG. Linear dependence between nodal powers in probabilistic a.c. load flow. Proc Inst Electr Eng 1977;124:529–34.
[32] Allan RN, Grigg CH, Newey DA, Simmons RF. Probabilistic power-flow techniques extended and applied to operational decision making. Ibid 1976;123(12):1317–24.
[33] Zeng X, Ren J, Wang Z, Marshall S, Durrani T. Copulas for statistical signal processing (Part I): Extensions and generalization. Signal Process 2014;94:691–702.

[34] Wu W, Wang K, Han B, Li G, Jiang X, Crow ML. A versatile probability model of photovoltaic generation using pair copula construction. IEEE trans sustain. Energy 2015;6(4):1337–45.
[35] Villanueva D, Feijóo AE, Pazos JL. An analytical method to solve the probabilistic load flow considering load demand correlation using the DC load flow. Electr Power Syst Res 2014;110:1–8.
[36] Leite da Silva AM, Arienti VL, Allan RN. Probabilistic load flow considering dependence between input nodal powers. IEEE Trans Power Appar Syst 1984;103(6):1524–30.
[37] Ruiz-Rodriguez FJ, Hernández JC, Jurado F. Probabilistic load flow for photo-voltaic distributed generation using the Cornish–Fisher expansion. Electr Power Syst Res 2012;89:129–38.
[38] Morales JM, Baringo L, Conejo AJ, Minguez R. Probabilistic power flow with correlated wind sources. IET Gener Transm Distrib 2010;4(5):641–51.
[39] Delgado C, Domínguez-Navarro JA. Point estimate method for probabilistic load flow of an unbalanced power distribution system with correlated wind and solar sources. Int J Electr Power Energy Syst 2014;61:267–78.
[40] Abdullah MA, Agalgaonkar AP, Muttaqi KM. Probabilistic load flow incorporating correlation between time-varying electricity demand and renewable power generation. Renew Energy 2013;55:532–43.
[41] Wang S, Zhang X, Liu L. Multiple stochastic correlations modeling for microgrid reliability and economic evaluation using pair-copula function. Int J Electr Power Energy Syst 2016;76:44–52.
[42] Stein M. Large sample properties of simulations using latin hypercube sampling. Technometrics 1987;29(2):143–51.
[43] Yu H, Chung CY, Wong KP, Lee HW, Zhang JH. Probabilistic load flow evaluation with hybrid Latin hypercube sampling and Cholesky decomposition. IEEE Trans Power Syst 2009;24(2):661–7.
[44] Owen AB. Latin supercube sampling for very high-dimensional simulations. ACM Trans Model Comput Simul (TOMACS) 1998;8(1):71–102.
[45] Glynn Peter W, Iglehart DL. Importance sampling for stochastic simulations. Manag Sci 1989;35(11):1367–92.
[46] Melchers RE. Importance sampling in structural systems. Struct Saf 1989;6(1):3–10.
[47] Cai D, Shi D, Chen J. Probabilistic load flow with correlated input random variables using uniform design sampling. Int J Electr Power Energy Syst 2014;63:105–12.
[48] Cui T, Franchetti FA. Quasi-Monte Carlo approach for radial distribution system probabilistic load flow. IEEE PES Int Conf Innov Smart Grid Technol (ISGT) 2013:1–6.
[49] Zhang L, Cheng H, Zhang S, Zeng P, Yao L. Probabilistic power flow calculation using the Johnson system and Sobol's quasi-random numbers. IET Gener Transm Distrib 2016;10(12):3050–9.
[50] Soleimanpour N, Mohammadi M. Probabilistic load flow by using nonparametric density estimators. IEEE Trans Power Syst 2013;28(4):3747–55.
[51] Rouhani M, Mohammadi M, Kargarian A. Parzen window density estimator-based probabilistic power flow with correlated uncertainties. IEEE Trans Sustain Energy 2016;7(3):1170–81.
[52] Allan RN, Al-Shakarchi MRG. Probabilistic a.c. load flow. Proc Inst Electr Eng 1976;123(6):531–6.
[53] Allan RN, Grigg CH, MRG Al-Shakarchi MRG. Numerical techniques in probabilistic load flow problems. Int J Num Methods Eng 1976;10(4):853–60.
[54] Allan RN, Al-Shakarchi MRG. Probabilistic techniques in a.c. load-flow analysis. Proc Inst Electr Eng 1977;124(2):154–60.
[55] Allan RN, Leite da Silva AM, Burchett RC. Evaluation methods and accuracy in probabilistic load flow solutions. IEEE Trans Power Appar Syst 1981;100(5):2539–46.
[56] Allan RN, Leite da Silva AM, Abu-Nasser AA, Burchett RC. Discrete convolution in power system reliability. IEEE Trans Reliab 1981;30(5):452–6.
[57] Sirisena HR, Brown EP. Representation of non-Gaussian probability distributions in stochastic load-flow studies by the method of Gaussian sum approximations. Proc Inst Electr Eng 1983;130(4):165–71.
[58] Valverde G, Saric AT, Terzija V. Probabilistic load flow with non-Gaussian correlated random variables using Gaussian mixture models. IET Gener Transm Distrib 2012;6(7):701–9.
[59] Kang C, Xia Q, Xiang N. Sequence operation theory and its application in power system reliability evaluation. Reliab Eng Syst Saf 2002;78(2):101–9.
[60] Prusty BR, Jena D. Sequence operation theory based probabilistic load flow assessment with photovoltaic generation. Michael Faraday IET Int Summit (MFIIS) 2015:1–6.
[61] Zhang N, Kang C, Singh C, Xia Q. Copula based dependent discrete convolution for power system uncertainty analysis. IEEE Trans Power Syst 2016;31(6):5204–5.
[62] Sanabria LA, Dillon TS. Stochastic power flow using cumulants and Von Mises functions. Int J Electr Power Energy Syst 1986;8(1):47–60.
[63] Zhang P, Lee ST. Probabilistic load flow computation using the method of combined cumulants and Gram-Charlier expansion. IEEE Trans Power Syst 2004;19(1):676–82.
[64] Usaola J. Probabilistic load flow in systems with wind generation. IET Gener Transm Distrib 2009;3(12):1031–41.
[65] Yuan Y, Zhou J, Ju P, Feuchtwang J. Probabilistic load flow computation of a power system containing wind farms using the method of combined cumulants and Gram-Charlier expansion. IET Renew. Power Gener 2011;5(6):448–54.
[66] Cramer H. Mathematical methods of statistics. Princeton University Press; 1999.
[67] Cai D, Chen J, Shi D, Duan X, Li H, Yao M. Enhancements to the cumulant method for probabilistic load flow studies. IEEE Power Energy Soc Gen Meet 2012:22–6.
[68] Williams T, Crawford C. Probabilistic load flow modeling comparing maximum entropy and Gram-Charlier probability density function reconstructions. IEEE Trans Power Syst 2013;28(1):272–80.
[69] Wu W, Wang K, Li G, Jiang X, Wang Z. Probabilistic load flow calculation using cumulants and multiple integrals. IET Gener Transm Distrib 2016;10(7):1703–9.
[70] Wan C, Xu Z, Dong ZY, Wong KP. Probabilistic load flow computation using first-order second-moment method. IEEE Power Energy Soc Gen Meet 2012:1–6.
[71] Rosenblueth E. Two-point estimates in probability. Appl Math Model 1981;5:329–35.
[72] Caro E, Morales JM, Conejo AJ, Minguez R. Calculation of measurement correlations using point estimate. IEEE Trans Power Deliv 2010;25(4):2095–103.
[73] Li KS. Point-estimate method for calculating statistical moments. J Eng Mech-ASCE 1992;118(7):1506–11.
[74] Harr ME. Probabilistic estimates for multivariate analysis. Appl Math Model 1989;13(5):313–8.
[75] Hong HP. An efficient point estimate method for probabilistic analysis. Reliab Eng Syst Saf 1998;59:261–7.
[76] Verbic G, Cañizares CA. Probabilistic optimal power flow in electricity markets based on a two-point estimate method. IEEE Trans Power Syst 2006;21(4):1883–93.
[77] Morales JM, Perez-Ruiz J. Point estimate schemes to solve the probabilistic power flow. IEEE Trans Power Syst 2007;22(4):1594–601.
[78] Caramia P, Carpinelli G, Varilone P. Point estimate schemes for probabilistic three-phase load flow. Electr Power Syst Res 2010;80(2):168–75.
[79] Soroudi A, Aien M, Ehsan M. A probabilistic modeling of photo voltaic modules and wind power generation impact on distribution networks. IEEE Syst J 2012;6(2):254–9.
[80] Zhao YG, Ono T. New point estimates for probability moments. J Eng Mech 2000;126(4):433–6.
[81] Mohammadi M, Shayegani A, Adaminejad H. A new approach of point estimate method for probabilistic load flow. Int J Electr Power Energy Syst 2013;51:54–60.
[82] Wang X, Gong Y, Jiang C. Regional carbon emission management based on probabilistic power flow with correlated stochastic variables. IEEE Trans Power Syst 2015;30(2):1094–103.
[83] Aien M, Fotuhi-Firuzabad M, Aminifar F. Probabilistic load flow in correlated uncertain environment using unscented transformation. IEEE Trans Power Syst 2012;27(4):2233–41.
[84] Ai X, Wen J, Wu T, Lee WJ. A discrete point estimate method for probabilistic load flow based on the measured data of wind power. IEEE Trans Indust Appl 2013;49(5):2244–52.
[85] Oke OA, Thomas DW, Asher GM, de Menezes LR. Probabilistic load flow for distribution systems with wind production using unscented transform method. IEEE PES Innov Smart Grid Technol (ISGT) 2011:1–7.
[86] Zou B, Xiao Q. Probabilistic load flow computation using univariate dimension reduction method. Int Trans Electr Energy Syst 2014;24(12):1700–14.
[87] Hong YY, Lin FJ, Yu TH. Taguchi method-based probabilistic load flow studies considering uncertain renewables and loads. IET Renew Power Gener 2016;10(2):221–7.
[88] Mohapatra A, Bijwe PR, Panigrahi BK. Unified boundary and probabilistic power flow. Electr Power Syst Res 2014;116:136–46.
[89] Mori H, Jiang W. A new probabilistic load flow method using MCMC in consideration of nodal Load correlation. 15th Int Conf Intell Syst Appl Power Syst 2009:8–12.
[90] Ren Z, Li W, Billinton R, Yan W. Probabilistic power flow analysis based on the stochastic response surface method. IEEE Trans Power Syst 2016;31(3):2307–15.
[91] Tang J, Ni F, Ponci F, Monti A. Dimension-adaptive sparse grid interpolation for uncertainty quantification in modern power systems: probabilistic power flow. IEEE Trans Power Syst 2016;31(2):907–19.
[92] Xu X, Yan Z. Probabilistic load flow evaluation considering correlated input random variables. Int Trans Electr Energy Syst 2016;26(3):555–72.
[93] Gupta N, Pant V, Das B. Probabilistic load flow incorporating generator reactive power limit violations with spline based reconstruction method. Elect Power Syst Res 2014;106:203–13.
[94] Prusty BR, Jena D. Combined cumulant and Gaussian mixture approximation for correlated probabilistic load flow studies: a new approach. CSEE J Power Energy Syst 2016;2(2):71–8.
[95] Wang Y, Pierrat L. Simulation of three-phase voltage unbalances using correlated gaussian random variables. 5th Int Conf Probabilistic Methods Appl Power Syst, Vanc, Br Columbia, Can 1997:515–20.
[96] Caramia P, Varilone P. Probabilistic AC/DC 3-phase load flow. 8th Int Conf Harmon Qual Power 1998:1018–28.
[97] Caramia P, Carpinelli G, Varilone P, Verde P. Probabilistic three-phase load flow. Int J Electr Power Energy Syst 1999;21(1):55–69.
[98] Wang YJ, Yang MJ. Probabilistic modeling of three-phase voltage unbalance caused by load fluctuations. IEEE Power Eng Soc Winter Meet 2000:2588–93.
[99] Wang YJ, Lambert P. A method integrating deterministic and stochastic approaches for the simulation of voltage unbalance in electric power distribution systems. IEEE Trans Power Syst 2001;16(2):241–6.
[100] Carpinelli G, Vito VD, Varilone P. Multi-linear Monte Carlo simulation for probabilistic three-phase load flow. Eur Trans Electr Power 2007;17(1):1–19.
[101] Caramia P, Carpinelli G, Pagano M, Varilone P. Probabilistic three-phase load flow for unbalanced electrical distribution systems with wind farms. IET Renew Power Gener 2007;1(2):115–22.
[102] Caramia P, Carpinelli G, Varilone P. Point estimate schemes for probabilistic three-phase load flow. Electr Power Syst Res 2010;80(2):168–75.
[103] Bracale A, Carpinelli G, Caramia P, Russo A, Varilone P. Point estimate schemes

for probabilistic load flow analysis of unbalanced electrical distribution systems with wind farms. 14th Int Conf Harmon Qual Power (ICHQP) 2010:26–9.
[104] Gomez-Gonzalez M, Ruiz-Rodriguez FJ, Jurado F. A binary SFLA for probabilistic three-phase load flow in unbalanced distribution systems with technical constraints. Int J Electr Power Energy Syst 2013;48:48–57.
[105] Alam MJE, Muttaqi KM, Sutanto D. A three-phase power flow approach for integrated 3-wire MV and 4-wire multigrounded LV networks with rooftop solar PV. IEEE Trans Power Syst 2013;28(2):1728–37.
[106] Ran X, Miao S. Three-phase probabilistic load flow for power system with correlated wind, photovoltaic and load. IET Gener Transm Distrib 2016;10(12):3093–101.
[107] Ho TK, Wang J, Leung KK, Tse CT, Sin LK. Probabilistic load flow calculation for AC traction supplies with at feeding. Proc Sixth Int Conf Adv Power System ControlOper Manag 2003:530–4.
[108] Ho TK, Chi YL, Wang J, Leung KK. Load flow in electrified railway [2nd International Conference on Power Electronics]. Mach Drives 2014:498–503.
[109] Ho TK, Chi YL, Wang J, Leung KK, Siu LK, Tse CT. Probabilistic load flow in AC electrified railways. IEE Proc Electr Power Appl 2005;152(4):1003–13.
[110] Yan P, Sekar A. Study of linear models in steady state load flow analysis of power systems. IEEE Power Eng Soc Winter Meet 2002;1:666–71.
[111] Dimitrovski A, Tomsovic K. Boundary load flow solutions. IEEE Trans Power Syst 2004;19(1):348–55.
[112] Leite da Silva AM, Arienti VL. Probabilistic load flow by a multilinear simulation algorithm. Proc Inst Electr Eng 1990;137(4):276–82.
[113] Brucoli M, Torelli F, Napoli N. Quadratic probabilistic load flow with linearly modeled dispatch. Int J Electr Power Energy Syst 1985;7(3):138–46.
[114] Eftekharnejad S, Vittal V, Heydt GT, Keel B, Loehr J. Impact of increased penetration of photovoltaic generation on power systems. IEEE Trans Power Syst 2013;28(2):893–901.
[115] IEEE . Standard for Interconnecting distributed resources with electric power systems [1547–2003]. IEEE Std 2003;1(28).
[116] Carpinelli G, Caramia P, Varilone P. Multi-linear Monte Carlo simulation method for probabilistic load flow of distribution systems with wind and photovoltaic generation systems. Renew. Energy 2015;76:283–95.
[117] Hollands KG, Huget RG. A probability density function for the clearness index, with applications. Sol Energy 1983;30(3):195–209.
[118] Tina G, Gagliano S, Raiti S. Hybrid solar/wind power system probabilistic modelling for long-term performance assessment. Sol Energy 2006;80(5):578–88.
[119] Jurado M, Caridad JM, Ruiz V. Statistical distribution of the clearness index with radiation data integrated over five minute intervals. Sol Energy 1995;55(6):469–73.
[120] Saunier GY, Reddy TA, Kumar S. A monthly probability distribution function of daily global irradiation values appropriate for both tropical and temperate locations. Sol Energy 1987;38(3):169–77.
[121] Ruiz-Rodriguez FJ, Hernandez JC, Jurado F. Probabilistic load flow for radial distribution networks with photovoltaic generators [International Conference on Power Engineering]. Energy Electr Drives (POWERENG) 2011:11–3.
[122] Hollands KG, Crha SJ. A probability density function for the diffuse fraction, with applications. Sol Energy 1987;38(4):237–45.
[123] King DL, Boyson WE, Kratochvil JA. Photovoltaic array performance model. Sandia National Laboratories, Albuquerque, New Mexico; 2004.
[124] Mukund RP. Wind and solar power systems. Boca Raton, FL, USA: CRC; 1999.
[125] Karaki SH, Chedid RB. Ramadan R. Probabilistic performance assessment of autonomous solar-wind energy conversion systems. IEEE Trans Energy Convers 1999;14(3):766–72.
[126] Aien M, Fotuhi-Firuzabad M, Rashidinejad M. Probabilistic optimal power flow in correlated hybrid wind–photovoltaic power systems. IEEE Trans Smart Grid 2014;5(1):130–8.
[127] Cai D, Li X, Zhou K, Xin J, Cao K. Probabilistic load flow algorithms considering correlation between input random variables: a review. IEEE 10th Conf Ind Electron Appl (ICIEA) 2015:1139–44.
[128] Papaefthymiou G, Kurowicka D. Using copulas for modeling stochastic dependence in power system uncertainty analysis. IEEE Trans Power Syst 2009;24(1):40–9.
[129] Liu PL, Kiureghian AD. Multivariate distribution models with prescribed marginals and covariances. Probabilistic Eng Mech 1986;1(2):105–12.
[130] Hoese A, Garcés F. Stochastic correlated simulation: an extension of the cumulant method to include time-dependent energy sources. Int J Electr Power Energy Syst 1999;21(1):13–22.
[131] Le DD, Pham KV, Ngo DV, Huynh KV, Nguyen NT, Berizzi A. An enhancement to cumulant-based probabilistic power flow methodologies. Smart Grid Technol-Asia (ISGTASIA) 2015:1–5.
[132] Oke OA, Thomas DW. Enhanced cumulant method for probabilistic power flow in systems with wind generation. 11th Int Conf Environ Electr Eng (EEEIC) 2012:849–53.
[133] Wang X, McDonald JR. Modern power system planning. London, U.K: McGraw Hill; 1994.
[134] Daily photovoltaic generation data. [Online]. Available: 〈https://www.pvoutput.org/ladder〉.
[135] Evans DL. Simplified method for predicting photovoltaic array output. Sol Energy 1981;27:555–60.
[136] Gulin M, Vašak M, Baotic M. Estimation of the global solar irradiance on tilted surfaces. 17th Int Conf Electr Drives Power Electron (EDPE) 2013:334–9.
[137] Daily ambient temperature data, Weather Underground. [Online]. Available: 〈https://www.wunderground.com/history〉.
[138] Solar irradiance data, SolarAnywhere. [Online]. Available: 〈https://www.solaranywhere.com〉.
[139] Pham DT, Dimov SS, Nguyen CD. Selection of K in K-means clustering [Proceedings of the Institution of Mechanical Engineers]. Part C: J Mech Eng Sc 2005;219(1):103–19.
[140] Power Systems Test Case Archive [Online], Available: 〈http://www.ee.washington.edu/research/pstca〉.